

The Fiskenæsset complex, West Greenland  
Part III

Chemistry of silicate and oxide minerals  
from oxide-bearing rocks, mostly from  
Qeqertarssuatsiaq

*by*

*I. M. Steele, F. C. Bishop, J. V. Smith and B. F. Windley*



# Grønlands Geologiske Undersøgelse

(The Geological Survey of Greenland)

Øster Voldgade 10, DK-1350 Copenhagen K

## Bulletins

- No. 111 Sand analysis as a method of estimating bedrock compositions in Greenland. 1974 by F. Kalsbeek, M. Ghisler & B. Thomsen. (*Meddr Grønland* 201,1). D.kr. 30.00
- No. 112 The structure of south Renland, Scoresby Sund – with special reference to the tectonometamorphic evolution of a southern internal part of the Caledonides of East Greenland. 1975 by B. Chadwick. (*Meddr Grønland* 201,2). D.kr. 42.00
- No. 113 Holocene history of the Greenland ice sheet based on radiocarbon-dated moraines in West Greenland. 1975 by N. W. Ten Brink. (*Meddr Grønland* 201,4). D.kr. 40.00
- No. 114 Ferri-sepiolite in hydrothermal calcite-quartz-chalcedony veins on Nûgssuaq in West Greenland. 1974 by K. Binzer & S. Karup-Møller. (*Meddr Grønland* 201,5). D.kr. 12.50
- No. 115 The Hurry Inlet granite and related rocks of Liverpool Land, East Greenland. 1975 by K. Coe. D.kr. 26.00
- No. 116 The crystal habit of naujakasite. 1975 by Ole V. Petersen and Steen Andersen. The crystal structure of naujakasite. 1975 by Riccardo Basso, Alberto Dal Negro, Antonio Della Giusta & Luciano Ungaretti. D.kr. 20.00
- No. 117 Organic compounds from the Rhaetic-Liassic coals of Scoresby Sund, East Greenland. 1975 by K. R. Pedersen & J. Lam. D.kr. 16.00
- No. 118 The South Qôroq Centre nepheline syenites, South Greenland. Petrology, felsic mineralogy and petrogenesis. 1976 by D. Stephenson. D.kr. 25.00
- No. 119 Carbonates et stromatolites du sommet du Groupe d'Eleonore Bay (Précambrien terminal) au Canning Land (Groenland oriental). 1976 par J. Bertrand-Sarfati & R. Caby. D.kr. 45.00
- No. 120 Early Tertiary flood basalts from Hareøen and western Nûgssuaq, West Greenland. 1976 by N. Hald. D.kr. 30.00
- No. 121 Early Silurian (Late Llandovery) rugose corals from western North Greenland. 1977 by R. A. McLean. D.kr. 46.00
- No. 122 Gardiner intrusion, an ultramafic complex at Kangerdlugssuaq, East Greenland. 1977 by W. Frisch & H. Keusen.
- No. 123 Stratigraphy, tectonics and palaeogeography of the Jurassic sediments of the areas north of Kong Oscars Fjord, East Greenland. 1977 by F. Surlyk.
- No. 124 The Fiskensæset complex, West Greenland Part III Chemistry of silicate and oxide minerals from oxide-bearing rocks, mostly from Qeqertarsuatsiaq. 1977 by I. M. Steele, F. C. Bishop, J. V. Smith & B. F. Windley.

Bulletins up to no. 114 were also issued as parts of *Meddelelser om Grønland*, and are available from Nyt Nordisk Forlag – Arnold Busck, Købmagergade 49, DK-1150 Copenhagen K, Denmark.

GRØNLANDS GEOLOGISKE UNDERSØGELSE  
Bulletin No. 124

The Fiskenæsset complex, West Greenland  
Part III

Chemistry of silicate and oxide minerals  
from oxide-bearing rocks, mostly from  
Qeqertarssuatsiaq

*by*

*I. M. Steele, F. C. Bishop, J. V. Smith and B. F. Windley*

1977

## Abstract

The textures and chemistry of silicates and oxides were investigated for 63 rocks from the Fiskenæsset complex, West Greenland, by light microscopy and electron microprobe analysis. Emphasis was placed on those chemical distributions known to depend on temperature.

Photomicrographs are given for the following intergrowths: spinel-magnetite, chromite-rutile, Cr-magnetite-Al-chromite. Magnetite occurs dispersed throughout Fe-bearing silicates, probably the result of oxidation. Chromite grains in chromitites commonly have a centre rich in inclusions of rutile and amphibole and a clean margin; partial recrystallization of the chromite followed by metamorphic equilibration to give a uniform composition from core to rim is indicated. Magnetite associated texturally with sulphides is Cr-free, and apparently results from oxidation.

Coexisting spinels outline a solvus between  $(\text{Fe}, \text{Mg})\text{Fe}_2\text{O}_4$  and  $(\text{Fe}, \text{Mg})\text{Al}_2\text{O}_4$  which has a critical point near  $(\text{Mg}, \text{Fe})(\text{Fe}_{0.6}\text{Al}_{0.6}\text{Cr}_{0.8})\text{O}_4$ . The wide tie-lines for Cr-poor specimens indicate equilibration below 500°C.

Coexisting ilmenite and ferromagnesian silicates apparently equilibrated in most rocks near  $650 \pm 100^\circ\text{C}$ , but in ones with late serpentine or tremolite, equilibration was probably below  $\sim 425^\circ\text{C}$ .

Coexisting pyroxenes apparently equilibrated at higher temperatures, either near 700 or  $850^\circ\text{C}$  depending on which laboratory calibration is used.

The Cr-rich spinels from the Fiskenæsset complex are lower in Mg than ones from dry basaltic stratiform complexes, and other chemical features lead to a distinctive composition range as proposed by Ghisler.

Further data for the silicates confirm most of the observations and conclusions in Part II, but (a) five specimens were found to contain tremolite apparently in compositional equilibrium with hornblende, (b) highly calcic plagioclase does not necessarily coexist with chromite as was proposed in Part II, (c) some specimens with unusually sodic plagioclase and unusually Fe-rich silicates may represent a cryptic differentiation trend.

Although many problems remain for further study, the silicates and oxides are interpreted as the variously metamorphosed products in the granulite, amphibolite or greenschist facies of a moderately wet Al-rich basaltic magma which underwent crystal-liquid differentiation under fairly oxidizing conditions. The original igneous assemblage apparently involved early precipitation of Mg-Al-Ti-Cr-magnetite, prolonged crystallization of highly calcic plagioclase and tschermakitic-magnesian-hornblende, and late crystallization of high-Fe, medium-Cr spinel.

### *Authors' addresses:*

I. M. Steele, J. V. Smith,  
Department of the  
Geophysical Sciences,  
University of Chicago,  
Chicago, Illinois,  
USA 60637

F. C. Bishop,  
Department of  
Geological Sciences,  
Northwestern University,  
Evanston, Illinois,  
USA 60201

B. F. Windley,  
Department of Geology,  
University of Leicester,  
LE1 7RH, England

## CONTENTS

Introduction .....	5
Analytical procedure and data .....	8
Textural descriptions .....	15
Chemistry and origin of opaque oxides .....	17
Solvus in the system $(\text{Mg,Fe})\text{Fe}_2\text{O}_4$ – $(\text{Mg,Fe})\text{Al}_2\text{O}_4$ – $(\text{Mg,Fe})\text{Cr}_2\text{O}_4$ .....	17
Single-phase Al-chromite and Cr-spinel .....	18
Magnetite and Cr-magnetite .....	18
Distribution of Mn between ilmenite and Cr-magnetite .....	20
Ti content of Cr-magnetite in relation to metamorphic grade .....	21
Distribution of MnO, NiO, MgO and $\text{TiO}_2$ between coexisting oxides .....	21
Primary chromites from zone Ch: comparison with other chromite data .....	22
Origin of chromites (and other spinel types) .....	24
Chemistry of silicates and relation to oxides .....	26
Amphibole chemistry .....	26
Pyroxene and olivine chemistry in relation to other minerals .....	27
Plagioclase chemistry .....	28
Silicate–oxide relations .....	28
Geothermometry using two pyroxenes and oxide–silicate .....	29
Two pyroxenes .....	29
Ilmenite–silicate and chromite–amphibole .....	31
General discussion and conclusions .....	32
Acknowledgements .....	34
Appendix .....	34
Petrographic notes on analyzed samples .....	34
References .....	37

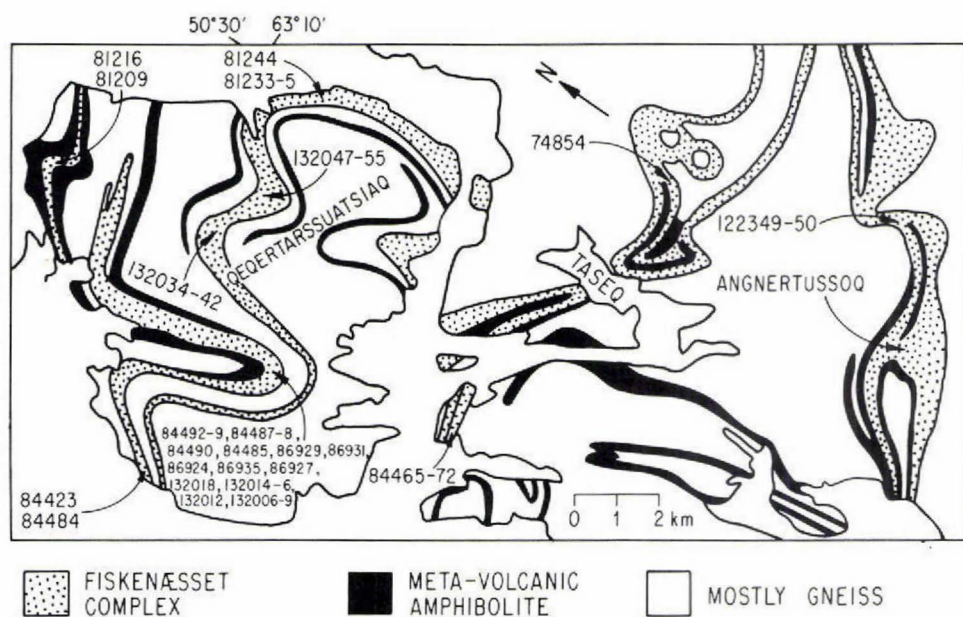


Fig. 1. Location of samples.

## INTRODUCTION

The literature on the Fiskenæsset complex, West Greenland, is growing rapidly as mineralogists, petrologists and geochemists exploit the opportunities provided by the high-grade metamorphism of an igneous complex apparently developed from crystal-liquid differentiation of a wet high-alumina basaltic magma.

Part I of this series (Windley *et al.*, 1973) described the stratigraphy, structure and whole-rock chemistry of part of the Fiskenæsset complex, while Part II (Windley & Smith, 1974) was a reconnaissance of the mineral chemistry made in response to the possibility that the Fiskenæsset rocks resemble those in the lunar crust. Although Ca-rich plagioclase occurs in both the Fiskenæsset and lunar anorthosites, the ubiquitous presence of amphibole in the former compared to the extreme dryness of the latter rules out any simple comparison. Indeed the rocks and minerals of the Fiskenæsset complex match much better with ones in the young Southern California batholith (Windley & Smith, 1976), thereby suggesting that at least the broad chemical and mineralogical features of the Fiskenæsset complex have nothing to do with its early age. Because of the complexity of the crystal-liquid differentiation processes of the presumed basaltic magma at Fiskenæsset, and because of the unresolved problems in the interpretation of lunar anorthosites, it is quite premature to make geochemical comparisons of planetary significance from simple comparison of Fiskenæsset and lunar rocks.

In this paper (Part III) we provide detailed chemical and textural data on silicates and oxides in selected Fiskenæsset rocks to provide a basis for estimates of the metamorphic conditions. A further paper (Part IV) will describe the sulphides. We emphasize that the rocks were deliberately chosen to yield a wide range of mineral assemblages, especially those suitable for geothermometry, and that they are biased toward ultramafic types. Furthermore they come from restricted areas of the complex and do not provide an overall geographic coverage. Part III overlaps slightly with, but largely complements, the comprehensive study of stratiform chromite deposits by Ghisler (1976) in which emphasis is placed on wide geographic coverage of chromite-bearing rocks of potential economic value. Some differences in results can be interpreted in terms of local variations in metamorphism and deformation, and serve as a warning that the Fiskenæsset complex is somewhat heterogeneous.

Since Part II, the following papers have appeared on the Fiskenæsset complex: annual reports and many papers in a report published by the Geological Survey of Greenland (Rapp. Grønlands geol. Unders. 73); Myers (1975) on igneous stratig-

raphy; Morgan *et al.* (1976) on volatile and siderophile trace elements; Henderson *et al.* (1976) on rare earth concentrations; Myers (1976a) on channel deposits; Myers (1976b) on tectonic interpretation of West Greenland rocks; and Myers & Platt (1977) on mineral chemistry which largely confirms our results of Part II.

The Fiskenæsset complex includes an early Precambrian layered and differentiated igneous suite ranging from minor ultramafic rocks through gabbros and leucogabbros to dominant anorthosites. This sequence occurs in high-grade amphibolites and gneisses as conformable layers up to about 2 km thick, and single layers can be followed along strike for up to 80 km. The complex was recrystallized by a hornblende-granulite grade of regional metamorphism that has a  $Pb^{204}/Pb^{206}$  whole rock age of  $2850 \pm 100$  m.y. (Black *et al.*, 1973). Retrograde metamorphism of amphibolite and greenschist grades as well as several periods of folding also affected the complex.

The main stratigraphic zones of the complex (originally labelled 2–8) are:

top	Upper Anorthosite (UA)
	Chromitite (Ch)
	Lower Anorthosite (LA)
	Upper Leucogabbro (ULG)
	Gabbro (G)
	Lower Leucogabbro (LLG)
bottom	Ultramafic Rocks (dunites, peridotites, pyroxenites) (UM)

The originally numbered zones 1 and 9 are amphibolites interpreted as metavolcanic rocks into which the complex was emplaced.

Because of primary lateral variations and effects of deformation, it is seldom possible to find all the main zones in any one traverse, and it is even less common to

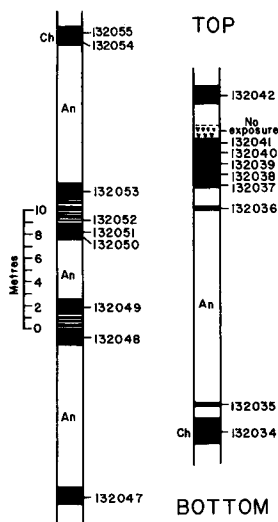


Fig. 2. Stratigraphy of two chromite sequences on east Qeqertarsuatsiaq island showing the position of analyzed samples.



Table 1. Mineralogy and rock type

Zone	Specimen Number	Rock Type	Sulphides											Oxides						Silicates									
			Pn	Po	Cp	Py	Mi	Hx	CP	Vi	Cb	Di	Il	Rt	Sp	Mt	CM	AC	Cm	Hb	Tr	Ac	At	Ol	Pl	Cp'	Op	Bi	Gt
UA	81244	An											x		x					x				x				x	x
	81235	An											x							x				x					
	81234	UM	x	x	x	x								x	x	x				x			x		x	x			
	81233	An		x		x														x				x					
Ch b	132042	Ch				x							x					x		x				x					
	132041	Ch				x	x											x		x				x					
	132040	Ch				x	x											x		x				x					
	132039	Ch											x					x		x				x					
	132038	Ch				x	x						x					x		x				x					
	132037	Ch				x	x						x					x		x				x				x	
	132036	Ch					x						x					x		x				x					
	132035	UM					x												x						x				
	132034	Ch	x										x					x		x					x				
Ch a	132055	Ch					x						x					x		x				x					
	132054	Ch											x					x		x				x					
	132053	Ch					x						x					x		x				x					
	132052	Ch				x	x	?					x					x		x				x				x	
	132051	Ch				x		?					x					x		x				x					
	132050	Ch					x						x					x		x				x					
	132049	Ch				x		x					x					x		x				x					
	132048	Ch					x						x					x		x				x					
	132047	Ch					x						x					x		x					x				
LA	132018	An																		x									
	132016	An																		x									
	86929	LG					x	x					x			x				x					x	x			
	84484	UM	x	x	x	x	x						x		x	x			x				x		x	x			
	74854	UM	x	x	x	x	x						x		x	x			x				x		x	x			
ULG	86931	LG				x	x								x					x					x		x		
	86924	LG				x	x						x			x				x					x				
	132015	G																		x					x				
	132014	LG																		x					x				
	132012	UM	x	x	x										x	x	x	x		x					x				
G	132009	G																		x					x		x		
	132008	G																	x						x				
	132006	G					x								x				x						x				
	84499	G			x	x	x								x				x						x				
	84498	G	x	x		x													x						x				
	84497	UM	x	x	x	x							x			x	x			x							x		
	84496	UM	x		x	x	x						x		x	x	x			x							x		
	84423	UM	x	x	x	x									x	x	x			x							x		
LLG	84495	LG													x	x	x			x					x	x	x		
	84494	UM	x	x	x	x										x	x	x							x				
	84493	LG														x				x					x		x		
	84492	UM	x	x	x	x										x				x						x			
	122350	UM	x	x									x		x		x			x					x		x		
	122349	UM	x	x	x								x		x		x			x					x		x		
UM	86935	UM	x	x	x	x										x				x						x		x	
	86927	UM	x	x	x	x														x						x		x	
	84490	UM	x	x	x								x		x				x						x		x		
	84488	UM	x	x	x								x		x				x						x		x		
	84487	UM	x	x	x								x		x				x						x		x		
	84485	UM	x	x	x								x		x				x						x		x		
	132007	UM	x	x	x								x		x				x						x		x		
	84472	UM	x	x	x	x							x						x										x <sup>b</sup>
	84471	UM						x	x							x	x			x					x		x		
	84470	UM														x	x			x					x		x		
	84469	UM	x	x	x												x			x					x		x		
	84468	UM	x					?	?						x	x	x			x					x		x		
	84467	UM	x					x	x							x	x	x		x					x		x		
	84466	UM	x	x	x											x	x			x					x		x		
	84465	UM	x			x	x									x	x			x					x		x		
81216	UM	x					?							x		x	x			x					x		x		
81209	UM	x	x	x					x	x			?			x	x			x						x	x		
-	132002	Am	x	x	x								x			x				x					x	x			

<sup>a</sup>also K-feldspar; <sup>b</sup>also quartz, Ac actinolite, AC Al-chromite, Am amphibolite, An anorthosite, At anthophyllite, Bi biotite, Cb cubanite, Ch chromitite, Cm chromite, CM Cr-magnetite, Cp chalcopyrite, Cp' clinopyroxene, CP Co-pentlandite, Di digenite, G gabbro, Gt garnet, Hb hornblende, Hx Heazlewoodite, Il ilmenite, LG leucogabbro, Mi millerite, Mt magnetite, Ol olivine, Op orthopyroxene, Pl plagioclase, Pn pentlandite, Po pyrrhotite, Py pyrite, Rt rutile, Sp spinel, Tr tremolite, UM ultramafic rock, Vi violarite. Serpentine occurs in 84470, 84468 and 84467, and epidote and muscovite occur in 132036 and 132052. A hydrated iron oxide, probably goethite (Go), occurs in 86929 and 132006.

find all the samples required for a particular study in any one traverse; therefore, the samples used in this study were chosen from several areas (fig. 1), but always with their stratigraphic position in mind.

Two chromitite sequences from the Ch zone were sampled about 2 km from each other, but on opposite sides (north and south respectively) of the repeated stratigraphy (for details of this stratigraphic repetition, see Part I). The sampling positions for these two chromitite sequences are illustrated in fig. 2; for both, the main zone is composed of alternating chromite-rich and anorthosite layers. In the thickest sequence (40 m), the total thickness of chromite-rich layers is about 10 m.

Table 1 lists the rock type for each specimen along with its minerals. Most rocks come from layers or lenses ranging from 0.3 to 2 m in thickness. In addition to the silicates already known from the complex, serpentine was found in three specimens from the UM zone (e.g. 84468, plate 1a) and tremolite was identified as a major constituent (30–40%) of 84465 (plate 1b) and as a very minor constituent of four other specimens (table 1). Furthermore, serpentine was found veining the entire rock 84470. Data are given for 132002 to illustrate the meta-volcanic rocks surrounding the complex.

In general the oxides magnetite, Cr-magnetite, spinel and ilmenite occur in the lower zones, and aluminian chromite and rutile in the upper zones. The nomenclature of the spinel-group minerals follows that used by Ghisler (1976, fig. 83), and the composition range of aluminian chromite (briefly Al-chromite) is more restricted than that for aluminous chromite as applied by Ghisler & Windley (1967). The terms spinel and spinel-type refer respectively to a  $\text{MgAl}_2\text{O}_4$ -rich phase and the general spinel group. Magnetite with more than  $\sim 3\%$   $\text{Cr}_2\text{O}_3$  is labelled Cr-magnetite. Whereas most Fiskensæset 'chromites' are Al-rich, that from 84472 has low  $\text{Al}_2\text{O}_3$  (7.4 wt. %), low MgO (0.5) and unusually high ZnO ( $\sim 1.6$ ).

## ANALYTICAL PROCEDURE AND DATA

Polished thin sections were cut for most specimens and studied by transmitted and reflected light microscopy. Electron microprobe analyses were made of selected grains to check for zoning and inter-grain variation. Several thousand routine analyses were made with a solid-state detector, and corrected by the Chicago 1976 system based on the Reed-Ware procedure programmed for an on-line computer. Analytical conditions were: 15 kV, beam current  $0.1\ \mu\text{A}$ , 1 or 2 minutes live time, spot size 0.25 to few  $\mu\text{m}$  diameter, detection level about 0.2 wt. % for Na-Zn ( $2\sigma$  level), accuracy 2–5% of amount present for major elements. Accurate analyses of oxides were made with spectrometers, mostly on grain mounts of concentrates of opaque oxides. The electron-probe (ARL-EMX) was operated at 15 kV and  $0.5\ \mu$  amp beam current for major elements (Cr, Fe, Mg) and 20 kV and  $1.0\ \mu$  amp for

Table 2. Electron microprobe analyses of silicates

	81244				81235			81234				81233		132042		132041		132040		132039		132038	
	Hb	Pl	Bi	Ga	Hb	Pl	Pl	Hb	Ol	Cp	Op	Hb	Pl	Hb	Pl	Hb	Pl	Hb	Pl	Hb	Pl	Hb	Pl
SiO <sub>2</sub>	41.8	48.4	36.7	39.7	42.4	46.7	55.5	47.0	40.3	52.2	56.0	42.9	49.3	45.1	47.2	44.0	46.1	44.7	46.8	43.8	47.8	44.7	47.2
TiO <sub>2</sub>	1.9	nd	3.0	nd	0.9	nd	nd	0.5	nd	nd	nd	1.9	nd	1.3	nd	1.0	nd	0.8	nd	1.4	nd	1.2	nd
Al <sub>2</sub> O <sub>3</sub>	14.3	32.9	15.9	22.6	12.8	34.2	28.9	11.1	nd	2.1	2.5	12.2	32.3	13.1	34.3	14.3	34.8	14.1	34.8	14.9	34.0	14.3	34.8
Cr <sub>2</sub> O <sub>3</sub>	nd	nd	nd	nd	nd	nd	nd	0.4	nd	nd	nd	nd	nd	1.5	nd	1.5	nd	1.7	nd	1.9	nd	1.7	nd
FeO	13.8	nd	13.4	25.1	16.1	nd	nd	5.6	13.2	2.6	9.5	17.0	nd	8.5	nd	9.3	nd	8.1	nd	6.8	nd	7.0	nd
MnO	nd	nd	nd	0.7	nd	nd	nd	nd	nd	nd	nd	nd	nd	0.2	nd	nd	nd	0.2	nd	nd	nd	0.2	nd
MgO	11.8	nd	15.4	9.7	10.0	nd	nd	18.0	46.5	16.3	31.9	10.1	nd	15.1	nd	14.1	nd	15.2	nd	15.3	nd	15.4	nd
CaO	11.4	16.3	nd	3.5	11.6	18.0	10.9	13.1	nd	25.1	0.2	11.5	15.8	11.0	17.2	11.3	17.7	11.2	17.4	11.6	16.4	11.3	17.3
Na <sub>2</sub> O	1.8	2.3	0.2	nd	1.4	1.6	5.9	1.4	nd	nd	nd	1.6	2.8	1.8	1.5	1.9	1.6	1.8	1.5	1.9	1.8	1.7	1.5
K <sub>2</sub> O	0.7	nd	9.4	nd	0.9	nd	nd	0.2	nd	nd	nd	1.2	nd	0.4	0.2	0.5	0.1	0.4	0.1	0.5	nd	0.5	0.1
Sum	97.5	99.9	94.0	101.3	96.1	100.5	101.2	97.3	100.0	98.3	100.1	98.4	100.2	98.0	100.4	97.9	100.3	97.4	100.6	98.1	100.0	98.0	100.9
	132037		132036		132035		132034		132055		132054		132053		132052		132051		132050		132049		
	Pl	Bi	Hb	Pl	Hb	Cp	Hb	Pl	Hb	Pl	Hb	Pl	Hb	Pl	Hb	Pl	Hb	Pl	Hb	Pl	Hb		
SiO <sub>2</sub>	44.6	37.3	43.5	48.5	45.9	52.7	43.6	48.7	44.1	46.0	44.8	45.7	44.5	46.0	43.6	46.9	45.3	46.9	44.6	46.7	45.3	45.3	
TiO <sub>2</sub>	nd	2.2	1.2	nd	1.5	0.3	1.4	nd	1.5	nd	1.4	nd	1.3	nd	1.2	nd	1.2	nd	1.3	nd	nd	1.2	
Al <sub>2</sub> O <sub>3</sub>	36.2	18.3	15.0	33.7	10.2	1.5	14.3	34.2	13.7	35.0	13.9	35.1	13.0	35.3	13.5	34.1	13.8	34.8	13.9	35.2	35.0	13.7	
Cr <sub>2</sub> O <sub>3</sub>	nd	1.0	1.5	nd	0.7	0.3	1.5	nd	1.7	nd	1.5	nd	1.7	nd	1.9	nd	1.4	nd	1.7	nd	nd	1.8	
FeO	nd	6.1	8.0	nd	12.9	9.1	8.4	nd	7.7	nd	6.1	nd	8.6	nd	10.3	nd	8.4	nd	8.4	nd	nd	6.5	
MnO	nd	nd	nd	nd	nd	0.2	0.2	nd	nd	nd	nd	nd	nd	nd	0.2	nd	0.2	nd	nd	nd	nd	0.2	
MgO	nd	20.0	14.9	nd	13.0	13.6	14.6	nd	15.1	nd	16.0	nd	14.7	nd	12.6	nd	14.3	nd	14.8	nd	nd	15.8	
CaO	19.3	nd	11.3	15.5	11.5	21.5	11.3	16.2	12.0	18.1	11.8	18.3	12.0	18.7	12.0	17.6	11.4	17.7	11.5	17.9	18.3	11.7	
Na <sub>2</sub> O	0.4	0.2	2.0	2.3	1.5	0.4	2.0	2.2	1.9	1.5	2.0	0.9	1.6	1.2	1.5	1.7	1.6	1.4	1.6	1.5	1.0	1.8	
K <sub>2</sub> O	0.2	10.2	0.5	0.1	1.0	nd	0.6	0.2	0.6	0.1	0.3	0.2	0.6	0.1	0.8	nd	0.4	nd	0.5	0.1	0.1	0.4	
Sum	100.7	95.3	97.9	100.1	98.2	99.6	97.9	101.5	98.3	100.7	97.8	100.2	98.0	101.3	97.6	100.3	98.0	100.8	98.3	101.4	99.7	98.4	
	132048		132047		132018		132016		86929		84484		74854		86931								
	Pl	Hb	Pl	Hb	Hb	Pl	Cp	Hb	Pl	Hb	Ol	Cp	Op	Hb	Ol	Cp	Op	Hb	Pl	Op			
SiO <sub>2</sub>	45.2	44.9	46.8	42.8	46.8	46.2	46.6	45.9	52.7	44.9	47.7	48.9	40.1	53.1	55.4	51.2	39.1	54.0	56.1	43.9	43.7	52.9	
TiO <sub>2</sub>	nd	1.1	nd	1.4	nd	0.6	nd	nd	1.3	nd	0.7	nd	nd	nd	0.4	nd	nd	nd	nd	nd	nd		
Al <sub>2</sub> O <sub>3</sub>	35.6	14.1	34.9	15.4	11.5	35.0	9.7	35.2	1.5	10.9	33.3	9.4	nd	1.6	1.8	6.4	nd	0.6	0.5	16.6	35.9	5.9	
Cr <sub>2</sub> O <sub>3</sub>	nd	1.8	nd	1.9	nd	nd	nd	nd	nd	nd	nd	nd	nd	nd	nd	nd	nd	nd	nd	nd	nd		
FeO	nd	6.5	nd	7.9	11.0	nd	14.7	nd	9.2	17.1	nd	5.8	17.7	3.4	12.1	6.1	22.5	4.3	14.1	8.0	nd	15.5	
MnO	nd	nd	nd	nd	nd	0.2	nd	nd	0.3	nd	0.2	0.3	nd	0.3	nd	nd	nd	0.3	nd	nd	0.2		
MgO	nd	15.8	nd	14.3	14.9	nd	12.1	nd	12.8	11.9	nd	18.3	42.6	16.2	29.9	18.9	38.8	16.7	29.0	14.7	nd	26.6	
CaO	18.4	11.6	17.6	11.8	10.9	18.2	12.1	18.9	23.5	8.3	16.4	12.8	nd	25.2	0.4	12.6	nd	24.2	0.3	11.7	19.9	0.3	
Na <sub>2</sub> O	0.7	1.7	1.3	1.8	1.2	1.1	0.6	nd	nd	1.3	2.2	1.3	nd	nd	0.3	0.9	nd	nd	0.3	1.8	0.2	0.3	
K <sub>2</sub> O	0.1	0.4	0.1	0.7	0.1	nd	0.6	1.2	nd	0.4	nd	0.1	nd	nd	nd	nd	nd	nd	0.2	nd	0.1		
Sum	100.0	97.9	100.7	98.0	96.4	100.5	97.2	101.2	99.7	96.4	99.6	97.5	100.7	99.5	100.2	96.5	100.4	99.8	100.6	96.9	99.7	101.8	

Table 2 cont.

	86924				132015*				132014				132012				132009				132008				132006															
	Hb		Pl		Hb		Op		Hb		Pl		Op		Hb		Pl		Op		Hb		Pl		Bi		KF†		Hb		Pl		Op							
SiO <sub>2</sub>	47.0	47.4	46.7	53.2	47.7	45.2	53.0	46.5	38.7	53.0	46.6	44.7	53.6	44.4	47.2	36.7	63.5	46.2	44.6	53.6																				
TiO <sub>2</sub>	2.5	nd	0.3	nd	nd	nd	nd	0.2	nd	2.7	0.3	nd	nd	0.7	nd	1.5	nd	nd	nd	nd																				
Al <sub>2</sub> O <sub>3</sub>	11.4	34.5	12.7	3.9	11.1	35.4	2.5	11.8	nd	nd	12.0	35.6	1.9	11.8	34.4	16.0	18.4	14.3	36.3	3.6																				
Cr <sub>2</sub> O <sub>3</sub>	nd	nd	0.1	nd	nd	nd	nd	nd	nd	nd	nd	nd	nd	1.6	nd	1.3	nd	nd	nd	nd																				
FeO	11.5	nd	9.1	16.2	9.5	nd	18.3	7.4	20.6	13.6	9.2	nd	19.1	12.2	nd	13.2	nd	7.1	nd	14.7																				
MnO	nd	nd	0.1	0.3	nd	nd	0.2	nd	0.3	0.2	nd	nd	0.2	0.2	nd	nd	nd	nd	nd	0.3																				
MgO	11.5	nd	15.9	26.3	15.8	nd	25.0	17.6	41.5	29.4	15.6	nd	24.7	12.1	nd	15.3	nd	15.5	nd	27.1																				
CaO	12.5	17.4	10.6	0.2	10.8	19.1	0.3	12.5	0.2	0.3	11.8	19.5	0.3	12.0	17.6	0.1	nd	11.8	19.9	0.3																				
Na <sub>2</sub> O	1.2	1.6	1.2	nd	1.4	0.8	nd	1.5	nd	0.1	1.7	0.6	nd	1.1	1.8	0.5	0.4	1.8	0.4	0.4																				
K <sub>2</sub> O	0.3	nd	0.2	nd	0.1	nd	nd	0.2	nd	nd	0.2	nd	nd	1.2	nd	9.3	16.6	nd	nd	nd																				
Sum	97.9	100.9	96.9	100.1	96.4	100.5	99.3	97.7	101.3	99.3	97.4	100.4	99.8	97.3	101.0	93.9	99.5	96.7	101.2	100.0																				
	84499				84498				84497				84496				84423				84495				84494				84493											
	Hb		Pl		Hb		Pl		Hb		Op		Hb		Op		Hb *		Op		Hb		Pl		Cp		Op		Hb		Op		Hb		Pl		Cp			
SiO <sub>2</sub>	41.9	47.2	43.6	44.1	48.5	40.3	55.8	47.2	53.6	49.8	39.8	53.2	54.4	47.2	46.8	52.7	52.7	48.4	55.2	47.3	45.7	51.7																		
TiO <sub>2</sub>	1.6	nd	0.6	nd	0.5	nd	nd	0.3	0.2	0.3	nd	nd	0.2	0.5	nd	nd	nd	0.3	0.2	0.5	nd	nd																		
Al <sub>2</sub> O <sub>3</sub>	13.7	33.8	15.4	36.5	9.4	nd	1.2	12.5	3.3	9.3	nd	2.3	2.8	10.0	34.0	1.1	1.3	9.7	1.9	9.8	35.1	1.1																		
Cr <sub>2</sub> O <sub>3</sub>	nd	nd	1.1	nd	0.8	nd	0.3	nd	nd	0.1	nd	nd	0.2	0.2	nd	nd	nd	nd	nd	nd	nd																			
FeO	18.3	nd	8.0	nd	4.7	13.4	9.4	6.4	11.7	6.6	17.1	3.3	11.5	11.8	nd	7.8	23.1	6.9	13.9	12.2	nd	8.1																		
MnO	nd	nd	nd	nd	nd	0.3	0.5	nd	0.4	0.1	0.4	nd	0.4	nd	nd	nd	0.5	0.2	0.4	nd	nd																			
MgO	8.3	nd	14.6	nd	19.2	47.0	32.9	16.7	30.5	18.5	42.8	16.9	31.2	14.0	nd	14.3	21.3	18.3	29.4	13.4	nd	13.3																		
CaO	11.2	16.9	12.3	19.7	12.4	0.2	0.2	12.1	0.4	13.1	0.2	24.6	0.3	11.8	17.6	22.6	0.4	12.4	0.5	12.4	18.4	23.5																		
Na <sub>2</sub> O	1.5	2.1	1.6	nd	1.3	nd	nd	1.2	nd	0.6	nd	nd	nd	1.0	1.5	0.4	0.5	1.6	0.1	1.0	1.2	0.5																		
K <sub>2</sub> O	1.2	nd	0.6	0.1	0.4	nd	0.1	0.4	nd	0.1	nd	nd	0.2	0.7	nd	nd	0.1	0.3	nd	0.7	nd	nd																		
Sum	97.7	100.0	97.8	100.4	97.2	101.2	100.4	96.8	100.1	98.5	100.3	100.3	101.2	97.2	99.9	98.9	99.9	98.1	101.7	97.3	100.4	98.2																		
	84492*				122350				122349				86935				86927				84490				84488															
	Hb		Op		Ol		Hb		Op		Hb		Op		Hb		Op		Hb		Ol		Op		Hb		Ol		Cp		Op		Hb		Ol		Cp		Op	
SiO <sub>2</sub>	46.1	53.2	37.5	50.5	38.5	55.6	52.1	37.7	55.5	50.1	54.0	55.7	49.1	40.1	56.5	50.4	39.5	54.6	54.8	47.2	38.7	53.7	55.4																	
TiO <sub>2</sub>	0.3	nd	nd	0.4	nd	nd	0.5	nd	nd	0.3	nd	nd	0.3	nd	nd	0.2	nd	nd	nd	0.8	nd	nd	nd																	
Al <sub>2</sub> O <sub>3</sub>	11.4	3.1	0.1	6.9	nd	0.8	6.0	nd	0.4	8.3	0.6	1.2	9.3	nd	1.5	7.9	nd	0.5	0.6	10.5	nd	0.7	0.8																	
Cr <sub>2</sub> O <sub>3</sub>	nd	nd	nd	nd	nd	nd	nd	nd	nd	0.5	nd	nd	0.9	nd	0.3	0.2	nd	nd	nd	0.5	nd	nd	nd																	
FeO	8.0	14.3	21.1	5.2	20.0	12.7	6.4	25.0	14.7	5.0	3.1	11.9	5.1	13.2	9.5	6.3	21.1	4.4	14.3	7.3	24.5	4.8	15.2																	
MnO	0.1	0.3	0.4	nd	nd	nd	nd	nd	nd	nd	nd	0.4	nd	0.2	0.2	nd	0.3	nd	0.3	nd	0.3	nd	0.3																	
MgO	17.1	28.9	39.6	19.6	41.3	30.3	20.1	40.0	28.9	19.0	17.0	30.9	19.6	46.4	32.2	19.4	41.2	16.8	29.3	17.2	38.1	16.1	28.1																	
CaO	12.3	0.4	0.3	12.0	nd	0.2	12.1	nd	0.4	12.6	24.7	0.2	12.4	nd	0.3	12.6	nd	24.1	0.3	12.7	nd	24.4	0.3																	
Na <sub>2</sub> O	1.2	nd	0.1	1.1	nd	nd	1.0	nd	nd	1.3	nd	0.2	1.2	0.2	0.2	1.2	nd	nd	0.2	1.9	nd	nd	nd																	
K <sub>2</sub> O	0.2	nd	nd	nd	nd	nd	nd	nd	nd	0.3	nd	nd	0.3	nd	nd	0.4	nd	nd	0.5	nd	nd	nd	nd																	
Sum	96.7	100.2	99.1	95.7	99.8	99.6	98.2	102.7	99.9	97.4	99.4	100.5	98.2	100.1	100.7	98.6	102.1	100.4	99.8	98.6	101.6	99.7	100.1																	

Table 2 cont.

	84487				84485			132007			84472			84471			84470			84469			
	Hb	Ol	Cp	Op	Hb	Cp	Op	Hb	Ol	Cp	Ac	At	Bi	Hb	Ol	Cp	Hb	Tr	Ol	Cp	Hb	Ol	Cp
SiO <sub>2</sub>	50.7	39.2	54.2	56.1	51.1	53.8	55.7	52.0	39.2	54.7	55.8	57.8	39.1	52.3	40.7	54.6	51.2	59.2	39.0	54.8	51.1	39.2	54.7
TiO <sub>2</sub>	0.5	nd	nd	nd	0.1	nd	nd	0.3	nd	nd	0.4	0.3	2.9	0.5	nd	0.7	0.5	nd	nd	0.5	0.5	nd	0.4
Al <sub>2</sub> O <sub>3</sub>	6.9	nd	0.1	0.5	7.2	0.7	0.8	6.0	nd	0.3	2.5	0.5	13.2	6.0	nd	nd	6.1	nd	nd	nd	6.4	nd	nd
Cr <sub>2</sub> O <sub>3</sub>	0.2	nd	nd	nd	nd	nd	nd	0.4	nd	nd	1.0	0.2	1.7	0.6	nd	nd	0.6	nd	nd	0.2	0.6	nd	nd
FeO	6.7	22.6	3.8	14.1	6.4	4.6	14.9	5.2	19.4	3.1	5.2	12.9	10.9	4.5	17.0	3.3	4.9	1.5	17.5	3.4	5.6	21.5	3.8
MnO	nd	0.3	nd	0.4	nd	nd	0.5	nd	0.4	nd	nd	0.4	nd	nd	0.3	0.2	nd	nd	0.5	nd	nd	0.4	nd
MgO	18.7	39.3	16.6	29.1	18.5	16.1	28.3	20.2	42.4	16.7	20.9	25.1	18.3	20.0	42.9	16.8	20.0	23.5	42.4	17.2	19.5	39.6	16.5
CaO	12.7	nd	24.5	0.4	12.9	24.3	0.3	12.8	nd	24.5	11.3	1.6	nd	13.4	nd	24.1	12.6	13.4	nd	23.7	12.2	nd	23.7
Na <sub>2</sub> O	1.3	0.2	nd	nd	0.8	nd	0.2	1.0	0.2	nd	0.3	nd	nd	1.2	nd	nd	1.1	nd	nd	nd	1.2	nd	nd
K <sub>2</sub> O	0.3	nd	nd	nd	0.1	nd	nd	nd	nd	nd	0.1	nd	9.1	0.3	nd	nd	0.2	nd	nd	nd	0.2	nd	nd
Sum	98.0	101.6	99.2	100.6	97.1	99.5	100.7	97.9	101.6	99.3	97.5	98.8	95.2	98.8	100.9	99.7	97.2	97.6	99.4	99.8	97.3	100.7	99.1
	84468				84467			84466			84465			81216				81209			132002		
	Hb	Ol	Cp	Op	Hb	Tr	Ol	Hb	Tr	Ol	Hb	Tr	Ol	Hb	Ol	Cp	Op	Hb	Cp	Op	Hb	Pl	Cp
SiO <sub>2</sub>	57.7	41.8	55.1	52.4	58.8	39.8	52.3	58.4	39.2	50.0	59.0	38.7	48.9	40.5	54.6	57.5	50.1	53.8	55.5	46.3	59.5	53.0	
TiO <sub>2</sub>	0.2	nd	0.5	0.6	0.2	nd	0.5	nd	nd	0.7	0.2	nd	0.9	nd	nd	nd	0.3	nd	nd	1.5	nd	nd	
Al <sub>2</sub> O <sub>3</sub>	1.2	nd	nd	5.7	nd	nd	4.9	nd	nd	7.8	0.7	nd	7.5	nd	0.1	0.3	8.8	1.0	1.6	9.8	25.6	1.4	
Cr <sub>2</sub> O <sub>3</sub>	0.3	nd	nd	0.7	nd	nd	0.4	nd	nd	0.3	nd	nd	0.2	nd	nd	nd	nd	nd	nd	0.2	nd	nd	
FeO	2.7	10.1	2.7	4.5	1.1	16.7	5.0	1.6	18.7	6.7	2.5	24.2	5.9	18.0	3.4	11.6	6.7	3.8	13.9	13.4	nd	8.8	
MnO	nd	0.8	nd	nd	nd	0.4	nd	nd	0.3	nd	0.2	0.3	nd	nd	nd	0.2	nd	nd	0.3	nd	nd	nd	
MgO	22.9	48.0	17.2	20.4	23.8	43.9	20.7	23.6	42.3	18.6	23.5	37.8	18.9	43.2	17.0	31.4	18.7	16.8	29.4	12.8	nd	13.2	
CaO	13.3	nd	24.3	12.5	13.8	0.2	12.6	13.8	0.1	12.2	12.9	0.1	12.4	nd	24.2	0.4	12.8	24.5	0.4	11.6	7.5	22.8	
Na <sub>2</sub> O	0.4	nd	nd	1.0	nd	nd	0.8	nd	nd	1.5	nd	nd	2.1	nd	nd	nd	0.9	nd	nd	1.8	7.2	0.5	
K <sub>2</sub> O	nd	nd	0.1	0.2	nd	nd	0.2	nd	nd	0.4	0.2	nd	0.4	nd	nd	nd	0.2	nd	nd	0.4	nd	nd	
Sum	98.7	100.7	99.9	98.0	97.7	101.0	97.4	97.4	100.6	98.2	99.2	101.1	97.2	101.7	99.3	101.4	98.5	99.9	101.1	97.8	99.8	99.7	

\*From part II. †Also BaO ~ 0.6; KF K-feldspar. For 81235 composition range of Pl is given. nd not detected.



Table 3. Electron microprobe analyses of oxide minerals

	81244		81235		81234		132042	132041	132040	132039	132038	132037	132036	132035	132034	132055	132054	132053
	Il	Mt	Il	Mt	CM	Sp	AC	AC	AC	AC	AC	AC	AC	AC	AC	AC	AC	AC
TiO <sub>2</sub>	52.8	0.5	51.6	1.4	0.2	nd	0.2	0.2	0.2	0.3	0.1	0.1	0.3	0.1	0.2	0.2	0.1	0.3
Al <sub>2</sub> O <sub>3</sub>	nd	0.4	0.2	0.3	1.1	54.3	23.9	25.2	28.3	26.7	25.1	18.8	25.2	23.8	22.7	24.3	26.6	18.8
Cr <sub>2</sub> O <sub>3</sub>	nd	0.3	nd	nd	7.5	9.8	33.0	31.8	31.2	33.8	34.2	32.7	32.5	33.1	32.1	36.4	33.0	37.6
Fe <sub>2</sub> O <sub>3</sub>	-	66.0	-	64.5	59.2	3.6	8.8	9.4	6.9	6.0	6.8	13.2	7.6	8.8	10.2	5.9	5.0	8.6
FeO	47.4	30.3	46.6	31.7	30.4	16.2	30.6	29.0	28.9	29.1	30.0	32.3	31.3	30.5	30.1	29.9	27.5	31.6
MnO	nd	nd	0.6	nd	nd	0.2	0.4	0.4	0.3	0.3	0.2	0.6	0.6	0.4	0.5	0.2	0.1	0.4
NiO	nd	nd	nd	nd	nd	0.7	0.2	0.1	0.1	0.2	0.1	0.1	0.1	0.1	0.1	0.1	0.2	0.1
MgO	nd	0.4	1.0	nd	0.5	16.1	3.6	4.8	5.2	5.0	4.3	1.6	3.2	3.6	3.7	4.3	5.6	2.7
Sum	100.2	97.9	100.0	97.9	98.9	100.9	100.7	100.9	101.1	101.4	100.8	99.4	100.8	100.4	99.6	101.3	98.1	100.1
	132052	132051	132050	132049	132048	132047	86929	84484	74854	132012								
	AC	Go	AC	AC	AC	AC	Il	Go	Il	Sp	CM	Il	Sp	CM	Sp	Mt	CM	AC
TiO <sub>2</sub>	0.7	0.2	0.2	0.1	0.1	0.2	47.7	nd	53.4	0.5	0.6	53.7	0.7	0.7	nd	0.2	1.1	0.3
Al <sub>2</sub> O <sub>3</sub>	17.3	24.8	24.5	26.3	27.9	22.8	0.1	0.5	0.2	62.5	1.0	0.1	60.4	0.7	64.2	0.5	3.7	30.6
Cr <sub>2</sub> O <sub>3</sub>	35.8	34.3	33.6	34.8	35.3	35.7	nd	nd	0.1	5.1	3.6	nd	4.6	3.2	nd	nd	15.4	25.8
Fe <sub>2</sub> O <sub>3</sub>	12.1	6.8	7.1	5.0	3.3	7.1	-	81.9	-	0.5	64.0	-	0.3	64.1	2.2	68.6	46.8	11.1
FeO	32.6	30.9	30.9	28.1	28.4	30.3	50.5	-	40.0	14.7	30.7	43.0	21.3	31.4	18.6	31.0	29.2	24.9
MnO	0.4	0.4	0.4	0.3	0.3	0.5	0.6	nd	2.1	0.2	nd	1.1	0.2	nd	0.2	nd	0.2	0.3
NiO	0.1	0.1	0.1	0.1	0.2	0.1	nd	2.7	nd	nd	0.3	-	0.2	nd	0.4	nd	0.5	0.2
MgO	1.4	3.6	3.3	5.5	5.6	3.5	1.1	0.4	4.9	18.4	0.7	2.8	13.8	0.4	15.7	0.3	0.9	8.2
Sum	100.4	101.1	100.1	100.2	101.1	100.2	100.0	85.5	100.7	101.9	100.9	100.7	101.5	100.5	101.3	100.6	97.8	101.4
	132008	132006	84499	84498	84497	84496	84495	84494	84493	84492								
	AC	Go	Il	Mt	AC	Il	CM	AC	Sp	Sp	CM	Sp	Mt	CM	Mt	CM	AC	Sp
TiO <sub>2</sub>	0.2	nd	50.0	0.2	nd	55.3	4.1	0.3	nd	nd	nd	0.2	nd	0.9	nd	9.4	0.2	nd
Al <sub>2</sub> O <sub>3</sub>	10.8	0.3	0.1	0.4	40.8	nd	3.6	31.0	64.7	50.2	0.9	62.8	0.4	0.3	0.3	3.4	28.6	64.0
Cr <sub>2</sub> O <sub>3</sub>	46.2	0.2	nd	0.2	20.0	0.3	16.8	25.8	0.7	9.9	8.1	2.4	0.4	2.2	0.2	16.1	26.0	nd
Fe <sub>2</sub> O <sub>3</sub>	10.2	80.5	-	68.8	4.4	-	40.6	10.2	1.7	6.8	28.0	2.0	67.9	65.1	67.5	33.0	11.1	4.1
FeO	32.7	-	46.3	31.2	26.4	37.6	33.2	24.5	16.3	19.0	58.0	17.7	30.4	31.4	30.2	38.6	23.4	18.6
MnO	0.7	0.2	0.9	nd	0.3	0.8	0.3	0.3	nd	nd	nd	0.2	nd	nd	nd	0.1	0.3	nd
NiO	nd	nd	nd	nd	0.1	nd	0.5	0.2	nd	nd	0.7	nd	nd	nd	0.4	0.5	0.2	nd
MgO	0.6	1.1	0.9	0.2	7.9	6.5	1.1	8.3	17.2	13.6	0.6	16.3	0.4	0.4	nd	nd	8.4	16.0
Sum	101.4	82.3	98.2	101.0	99.9	100.5	100.2	100.6	100.6	99.5	96.3	101.6	99.5	100.3	98.6	101.1	98.2	102.7

Table 3 cont.

	122350			122349		86935		86927		84490			84488			84487			
	Il	Sp	CM	Il	CM	AC	CM	AC		Il	Sp	CM	Il	Sp*	CM	Il	CM		
TiO <sub>2</sub>	52.6	1.1	1.0	51.7	4.3	0.3	1.5	0.2		52.8	0.4	1.9	52.8	0.3	1.6	53.4	2.9		
Al <sub>2</sub> O <sub>3</sub>	nd	49.5	2.3	nd	5.4	25.6	3.0	29.2		0.2	49.9	4.2	nd	47.2	2.4	nd	3.0		
Cr <sub>2</sub> O <sub>3</sub>	nd	13.8	9.0	nd	4.8	31.3	19.0	29.0		nd	12.6	8.7	nd	15.0	8.2	0.2	9.7		
Fe <sub>2</sub> O <sub>3</sub>	-	1.1	56.9	-	51.5	10.7	43.6	10.1		-	2.6	53.0	-	1.6	55.7	-	51.3		
FeO	42.2	22.2	30.9	44.6	32.6	27.0	30.1	23.3		42.5	22.9	31.4	43.3	23.4	32.2	42.3	32.7		
MnO	1.2	0.4	0.3	0.5	0.3	0.5	0.4	0.3		1.6	0.4	0.2	1.0	nd	nd	1.2	0.4		
NiO	nd	0.4	0.3	nd	nd	nd	0.5	nd		nd	-	nd	nd	nd	nd	nd	0.3		
MgO	<u>3.9</u>	<u>11.8</u>	<u>0.9</u>	<u>3.0</u>	<u>2.2</u>	<u>6.1</u>	<u>1.4</u>	<u>8.8</u>		<u>3.3</u>	<u>11.1</u>	<u>1.1</u>	<u>3.0</u>	<u>10.3</u>	<u>0.7</u>	<u>3.6</u>	<u>0.9</u>		
Sum	99.9	100.3	101.6	99.8	101.1	101.5	99.5	100.9		100.4	99.9	100.5	100.1	99.8	100.8	100.7	101.2		
	84485			132007		84472				84471			84470			84469			
	Il	Sp	CM	CM	Il	CM	Il	Mt	CM†	Il	Mt	CM	Il	Mt	CM	Il	CM		
TiO <sub>2</sub>	53.0	0.3	0.8	2.6	51.2	2.5	51.3	2.0	nd	49.8	nd	0.8	53.2	0.2	1.1	54.3	1.6		
Al <sub>2</sub> O <sub>3</sub>	0.1	56.7	1.2	1.7	0.4	3.8	nd	0.5	7.4	0.1	0.3	0.4	nd	nd	0.3	nd	0.8		
Cr <sub>2</sub> O <sub>3</sub>	nd	5.9	4.3	3.1	0.3	15.2	nd	0.1	58.1	0.1	0.2	18.8	nd	0.8	16.1	nd	11.8		
Fe <sub>2</sub> O <sub>3</sub>	-	0.9	62.4	57.6	-	45.0	-	65.5	0.9	-	69.0	49.7	-	67.2	51.8	-	54.0		
FeO	42.2	21.8	31.4	30.4	42.9	31.8	45.7	29.9	32.2	46.1	30.3	31.0	42.8	30.1	31.5	42.2	32.2		
MnO	2.5	0.4	nd	0.3	1.3	0.4	1.3	nd	nd	1.4	nd	0.5	1.6	nd	0.3	1.7	nd		
NiO	nd	0.2	nd	nd	nd	nd	nd	0.1	nd	nd	nd	nd	nd	nd	nd	nd	nd		
MgO	<u>2.6</u>	<u>12.3</u>	<u>0.5</u>	<u>1.4</u>	<u>3.2</u>	<u>1.3</u>	<u>0.3</u>	<u>0.4</u>	<u>0.5</u>	<u>2.2</u>	<u>0.6</u>	<u>0.8</u>	<u>2.9</u>	<u>0.5</u>	<u>0.7</u>	<u>2.7</u>	<u>0.6</u>		
Sum	100.4	99.5	100.6	97.1	99.3	100.0	98.6	98.5	100.7	99.7	100.4	102.0	100.5	98.8	101.8	100.9	101.0		
	84468			84467			84466			84465			81216		81209				
	Il	Mt	CM	Il	Mt	CM	AC	Il	Mt	CM	Il	Mt	CM	Il	CM	Il?	Mt	CM	Sp
TiO <sub>2</sub>	53.3	nd	0.2	51.8	nd	0.8	1.8	54.6	0.5	4.6	51.3	0.3	2.4	53.4	1.8	42.9	0.4	2.6	0.2
Al <sub>2</sub> O <sub>3</sub>	nd	nd	nd	nd	nd	nd	8.0	nd	0.2	2.8	nd	nd	0.2	0.7	1.9	1.61	nd	2.0	49.8
Cr <sub>2</sub> O <sub>3</sub>	nd	0.2	4.3	nd	nd	20.4	31.3	nd	0.4	17.9	nd	nd	3.2	0.4	7.7	5.62	0.8	8.2	11.3
Fe <sub>2</sub> O <sub>3</sub>	-	68.3	64.6	-	69.2	47.1	26.5	-	67.7	39.2	-	68.3	62.2	-	56.4	-	67.1	54.5	3.6
FeO	39.8	30.4	30.7	42.3	30.6	30.4	30.7	39.1	30.7	33.7	45.7	31.2	32.9	40.8	31.2	44.4	31.2	32.5	19.4
MnO	4.4	nd	nd	2.6	nd	0.5	1.1	1.8	nd	0.5	1.3	nd	0.3	1.1	0.2	3.56	nd	0.3	nd
NiO	nd	nd	nd	nd	nd	nd	nd	nd	nd	nd	nd	nd	nd	nd	0.3	nd	nd	nd	nd
MgO	<u>2.3</u>	<u>0.3</u>	<u>0.4</u>	<u>3.4</u>	<u>0.4</u>	<u>0.7</u>	<u>2.1</u>	<u>4.2</u>	<u>0.6</u>	<u>1.2</u>	<u>0.3</u>	<u>nd</u>	<u>0.5</u>	<u>4.7</u>	<u>1.1</u>	<u>0.83</u>	<u>nd</u>	<u>0.9</u>	<u>13.0</u>
Sum	99.8	99.2	100.2	100.1	100.2	99.9	101.5	99.7	100.1	99.9	98.6	99.8	101.7	101.1	100.6	98.92	99.5	101.0	97.3

\* ~ 2% ZnO † ~ 1.6% ZnO nd not detected

other elements, using a fine spot (up to few  $\mu\text{m}$  diameter). Analyses are accurate to 2–5% of amount present for concentrations down to 1 wt. %, and the detection level ( $1\sigma$ ) for minor elements is near 0.02 wt. %. Matrix corrections were made using computer program EMPADR VII (Rucklidge, 1967) which is based on the correction procedures outlined by Sweatman & Long (1969). Standards were as follows: Mg, Ca, Si diopside glass with 2%  $\text{TiO}_2$ ; Al-synthetic  $\text{MgAl}_2\text{O}_4$ ; Ti-natural ilmenite (Ti 29.73, Fe 36.64, Mn 0.66, Mg 0.60); Cr-natural chromite (Cr 17.23, Fe 40.6, Al 5.08, Mg 4.28, Ti 1.2); Mn-hortonolite (Mn 3.64); Ni-olivine (Ni 0.33); Fe-Fe metal. Major elements (Cr, Fe, Mg) were analyzed simultaneously and points marked on a photograph. Other elements were analyzed by relocating these points. Individual backgrounds were determined for the minor elements. Vanadium was not analyzed but definitely occurs in some oxide minerals at the 0.0x to 0. x wt. % level, as shown by Ghisler (1976) for chromites.

Tables 2 and 3 list representative analyses for the silicates and oxides in the specimens of table 1. Some variations in analyses were found from grain to grain but the variations were too small (0 to few % of amount present of major elements) to warrant detailed tabulation. Table 4 shows that even the variations of analyses from chromite, which occurs as both poikilitic and inclusion-free grains, are close to experimental error.

*Table 4. Analyses of chromite*

	132050				132053			
	mp	ep	mp	ec	mp	ec	mp	ec
$\text{Al}_2\text{O}_3$	21.5	21.4	23.7	23.1	16.9	17.5	16.7	15.9
$\text{Cr}_2\text{O}_3$	36.0	35.4	33.5	33.7	35.8	35.6	36.3	38.1
FeO	38.0	37.9	36.5	37.8	41.4	42.1	42.1	40.6
MgO	3.4	3.3	3.9	3.5	2.7	3.0	2.8	2.7
	132038				132037			
	ec	b	mp	mp	b	ec	mp	ec
$\text{Al}_2\text{O}_3$	25.4	24.8	25.0	24.7	24.8	24.9	25.2	24.7
$\text{Cr}_2\text{O}_3$	33.1	33.4	33.7	33.1	33.6	33.7	28.8	29.1
FeO	36.5	36.6	36.9	37.1	37.5	36.8	41.0	41.0
MgO	4.9	4.8	4.8	4.7	5.0	4.6	3.1	2.9
	132054				132055			
	c	p	c	p	c	p	c	p
$\text{Al}_2\text{O}_3$	28.7	28.7	28.5	29.7	22.3	22.8	23.3	23.4
$\text{Cr}_2\text{O}_3$	32.9	33.0	32.6	32.5	34.2	34.6	34.1	34.0
FeO	31.9	31.5	32.3	31.7	38.5	37.8	37.6	37.5
MgO	6.6	6.4	6.4	6.6	4.0	3.9	4.1	4.1

b, boundary between clear (c) and poikilitic (p); m middle and e edge of same grain; single bar separates data for different grains.

## TEXTURAL DESCRIPTIONS

Plate 1c–1e illustrates selected relationships between silicates and oxides. All were taken in transmitted light, and show an area 0.6 mm across.

The oxides are largely associated with the mafic silicates. In ultramafic rocks, spinel-magnetite intergrowths occur as dense concentrations of granules of varying sizes within and between silicates.

In chromitites, Al-chromite grains are closely associated with hornblende (plate 1c) and rarely with biotite and plagioclase (plate 1d). Commonly Al-chromite forms subidiomorphic grains in a mafic silicate matrix, and the fine scale banding is consistent with a cumulus origin. Rarely there is a second population of fine-grained chromite (plate 1c). In reflected light, the coarse chromite grains characteristically show a poikilitic centre with amphibole inclusions and a clean margin, but various ratios of clean to poikilitic areas can be found even in the same thin section. Detailed discussion is given later.

Magnetite and Cr-magnetite occur both as coarse interstitial grains between and as fine dust-like inclusions in silicate grains (plate 1e).

Plates 2 and 3 show the complex relations between coexisting oxides. All these plates were taken with reflected light from heavy grains mounted in epoxy (matte grey).

Spinel-magnetite intergrowths in silicates of ultramafic rocks are illustrated in plates 2a–2e. The textures vary from (a) coexistence of one grain of spinel and one grain of magnetite in each composite inclusion (plates 2a, b) to (b) small magnetite grains at the boundary of a dominant spinel grain (plates 2c, d). Incomplete movement of magnetite to the grain boundary is indicated in plate 2c where the central part of the spinel is peppered with magnetite inclusions. That the outer part is free of inclusions can be explained by migration of magnetite to the outer boundary of the spinel with the silicate. The texture correlates with the size of the spinel grain, and only the larger grains retain the central poikilitic zone. Plate 2b shows oriented darts, probably of spinel, in that part of the magnetite grain remote from contact with the coarse spinel; again there is a 'shadow zone' attributable to diffusion-controlled migration of the spinel component from the magnetite.

Chromite-rutile intergrowths are present in nearly all rocks from zone Ch, with rutile amounting to only ~1%. Plate 2e shows the typical occurrence of rutile as small highly-reflecting grains either within the chromite or at grain boundaries.

Particularly important is the distinction between areas of chromite rich in inclusions of silicates and rutile and areas free of such inclusions. Most chromite grains

consist of a central poikilitic region and an outer clean region (plate 2e). Ghisler (1970) had also noted two types of chromite textures from the Fiskenæsset complex: (a) a 'clean' chromite with only rutile exsolution, (b) a chromite with numerous silicate inclusions as well as rutile. His earlier tentative interpretation that the former was primary and the latter was a secondary overgrowth during igneous sedimentation was replaced (1976) by the concept of partial metamorphic recrystallization in which "the chromite grains were cleaned of silicate inclusions and became relatively enriched in both divalent and trivalent iron with a corresponding distinct decrease in Mg and Al and a slight decrease in Cr". We endorse the concept of metamorphic recrystallization which fits also with magnetite-spinel textures described earlier. However, our samples do not show the chemical differences between poikilitic and clean chromite (table 4), and we suggest that Ghisler's samples did not undergo as strong a metamorphic equilibration after partial recrystallization as did ours. The two sets of samples come from different traverses in the complex and further study is desirable to relate texture, chemistry and rock deformation over the entire complex.

Two samples (132037 and 132052) with essentially no rutile are the only chromites with substantial biotite, and they have chromites of unusual composition.

In the LLG, G and ULG, several examples (132012, 84494, 84497) of Cr-magnetite (Cr-*mt*) and Al-chromite (Al-*chr*) intergrowths occur as illustrated in plate 3a-c. Al-chromite is the more abundant phase but Cr-magnetite often makes up 10–20% of the opaque phases. Complex subsolidus reactions occurred between these phases. Plate 3a shows numerous 'trails' of Cr-magnetite in an Al-chromite host; some structural control, probably from cracks or other defects, is recognizable. Plate 3b shows a high magnification image of one of the 'trails' of plate 3a. The Al-chromite no longer appears homogeneous but instead has numerous bright inclusions which are not observed in a band bordering the bright 'trail'; presumably, the bright phase has precipitated along a line defect and depleted the host of this component. Electron-probe analysis showed that the bright trail is Cr-magnetite; however, plate 3b shows that the Cr-magnetite actually consists of at least four oriented components. Optical study suggests that rutile and two silicates may be present; unfortunately the scale of this intergrowth is not resolvable with the electron-microprobe. In plate 3c the Cr-magnetite occurs only at grain boundaries and fractures and shows no evidence of breakdown. Chemical evidence in the next section suggests that these intergrowths once constituted a homogeneous Al-chromite.

In all zones except Ch there is a further common type of intergrowth involving minor ilmenite associated with either Cr-magnetite, Cr-magnetite low in  $\text{Al}_2\text{O}_3$ , or both.

Magnetite and Cr-magnetite commonly occur as small grains dispersed throughout Fe-bearing silicate grains, and the texture suggests derivation by oxidation. Cr-magnetite was found as nearly -parallel ellipsoidal to elongated polygonal grains



with fine spinel (?) lamellae in a hornblende host (plate 3d). Graphic intergrowths of magnetite and orthopyroxene, along with minor spinel are illustrated in plate 3e.

## CHEMISTRY AND ORIGIN OF OPAQUE OXIDES

This section evaluates the chemistry of the oxides, and attempts to provide an estimate of the conditions of crystallization and of the degree of subsolidus reactions. We describe three spinel occurrences: coexisting Cr-magnetite and Cr-spinel; single phase Al-chromite and Cr-spinel; and magnetite and Cr-magnetite with low  $\text{Al}_2\text{O}_3$ . The division, while based on chemistry, is also related to the stratigraphy of the intrusion.

### Solvus in the system $(\text{Mg, Fe})\text{Fe}_2\text{O}_4$ – $(\text{Mg, Fe})\text{Al}_2\text{O}_4$ – $(\text{Mg, Fe})\text{Cr}_2\text{O}_4$

The major part of the composition of a spinel-type phase can be plotted in the above system while ignoring the minor elements Ni, Mn and Ti and the variation of the  $\text{Fe}^{+2}/\text{Mg}$  ratio. Coexisting Al-bearing spinels with  $(\text{Mg, Fe})\text{Al}_2\text{O}_4 > \sim 1 \text{ mol } \%$  occur in all zones except Ch, and show a consistent pattern outlining a solvus in the above ternary system with tie-lines approximately parallel to the  $(\text{Mg, Fe})\text{Fe}_2\text{O}_4$ – $(\text{Mg, Fe})\text{Al}_2\text{O}_4$  join (fig. 3). As the Cr content increases, the coexisting compositions approach each other. Several samples, including 84467, 84498, and all those from zone Ch, show one spinel phase and thus place a limit on the solvus at approximately  $(\text{Mg, Fe})\text{Fe}_{0.6}\text{Al}_{0.6}\text{Cr}_{0.8}\text{O}_4$  for the temperature of equilibration for these samples. Other studies (Muir & Naldrett, 1973; Springer, 1974; Irvine, 1974a) have also recognized this relationship and the published data (fig. 3) closely match those from Fiskensæset.

Turnock & Eugster (1962) outlined a solvus in the system  $\text{FeAl}_2\text{O}_4$ – $\text{FeFe}_2\text{O}_4$  (temperatures indicated on base of fig. 3). In this study, the oxygen fugacity was controlled by the  $\text{Fe}_2\text{SiO}_4$ – $\text{Fe}_3\text{O}_4$ – $\text{SiO}_2$  buffer, and the coexistence of silicates with the spinels at Fiskensæset should guarantee a similar level of oxidation. The Fiskensæset spinels with the lowest Cr-substitution show a mutual solubility of about 2% of either  $(\text{Fe, Mg})\text{Fe}_2\text{O}_4$  or  $(\text{Fe, Mg})\text{Al}_2\text{O}_4$ . This is lower than the smallest amounts found by Turnock & Eugster (their lowest, reliable experimental points are for  $600^\circ\text{C}$ ), but extrapolation suggests that the Fiskensæset assemblages equilibrated below  $500^\circ\text{C}$ , and perhaps as low as  $350^\circ\text{C}$ . These temperatures should be treated cautiously as it is difficult to obtain true equilibrium for a solvus at low temperature. Cremer (1969), based on experimental work on the other joins, proposed that the solvus projects (in the Mg-free system) form the  $\text{FeCr}_2\text{O}_4$ – $\text{FeAl}_2\text{O}_4$  join, but this is inconsistent with the data of fig. 3, as first pointed out by Muir & Naldrett (1973). Based on the above discrepancy we suggest that the diagram of

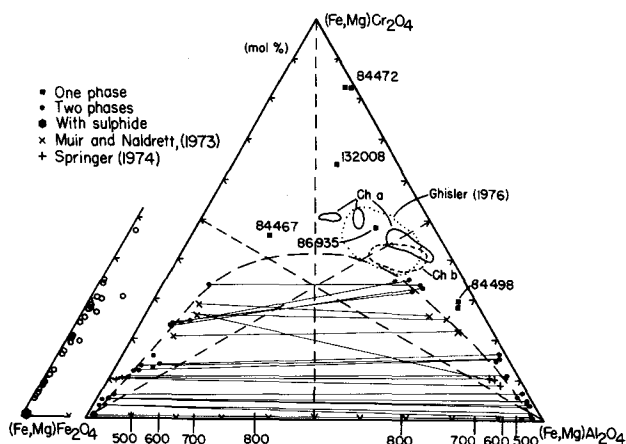


Fig. 3. Plot of Al-bearing ( $\text{Al}_2\text{O}_3 > \sim 2\%$ ) spinel-type compositions of Fiskensæset samples in the ternary system  $(\text{Mg,Fe})\text{Cr}_2\text{O}_4$ . Sub-diagram at left shows spinel-types with  $\text{Al}_2\text{O}_3 < \sim 2\%$  which plot nearly on the magnetite-chromite join. Coexisting compositions are joined in the main diagram, and these outline a solvus (drawn by eye) projecting into the ternary system from the  $(\text{Mg,Fe})\text{Fe}_2\text{O}_4$ – $(\text{Mg,Fe})\text{Al}_2\text{O}_4$  join. Published data (Springer,

1974; Muir & Naldrett, 1973) for coexisting spinels fall close to this solvus. Only generalized areas are shown for zones Ch a and Ch b and for data of Ghisler (1976). Turnock & Eugster (1962) experimentally determined the solvus in the  $\text{FeFe}_2\text{O}_4$ – $\text{FeAl}_2\text{O}_4$  system and their temperatures are indicated on the base of the ternary diagram.

Cremer (1966) cannot be used for estimating the crystallization temperatures of chromites (e.g. Ghisler, 1976).

### Single-phase Al-chromite and Cr-spinel

These are mainly restricted to zone Ch, but there are minor occurrences in lower zones. Their compositions are shown on figs 3, 4 and 5. Data for chromites from zones Ch a and b match the generalized compositional range of Ghisler (1976, his Table A-13) with the exception that his banded type tends to have higher values of both  $\text{Fe}^{+2}$  and  $\text{Fe}^{+3}$ .

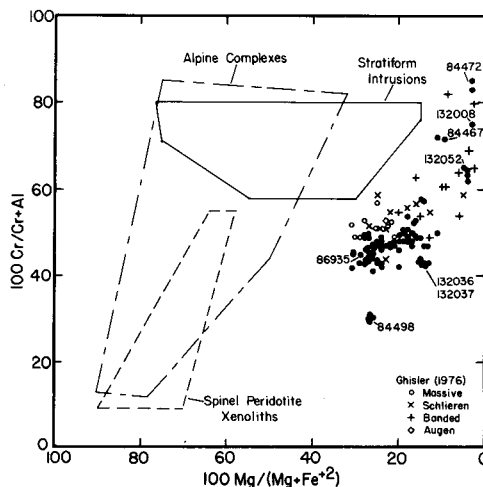
The solvus in fig. 3 is based on coexisting spinels readily observed by light microscopy, and must represent a temperature at which diffusion was effective over the scale of the texture. The very fine complex textures observed at the limit of optical microscopy (plate 3b) may represent an even wider exsolution gap for a lower temperature at which diffusion is very sluggish. Electron microscopic studies are highly desirable to test whether zone Ch chromites actually lie inside a low-temperature solvus.

In lower zones the spinel-types occur as minor interstitial grains in gabbros (132008, 84498) and ultramafic rocks (84467, 84472, 86935). Compositionally these are diverse and show few similarities on figs 3–5.

### Magnetite and Cr-magnetite

These types, when low in  $\text{Al}_2\text{O}_3$ , (fig. 3, open circles), occur in all rock types (AN, LG, G, UM; table 1) and in all zones except Ch. Compositions (fig. 3) range

Fig. 4. Comparison of  $mg$  v.  $cr$  for Fiskensæset spinels with generalized ranges for alpine-type complexes, stratiform dry basaltic intrusions and spinel peridotite xenoliths (Irvine, 1974a). Only those Fiskensæset spinels with  $Al_2O_3 > 2$  wt.% are plotted: present data, filled circles; Ghisler 1976, Table A 13), other symbols based on textural classification.  $mg$  is  $100 Mg/(Mg + Fe^{2+})$  atomic, and  $cr$  is  $100 Cr/(Cr + Al)$ .



from virtually pure magnetite ( $Cr_2O_3 < 0.2$  wt. %) to magnetite with  $\sim 30$  mol % chromite. In some rocks two types of Cr-magnetite coexist, usually with ilmenite; these two types have different Cr contents and are described as high-Cr and low-Cr varieties of Cr-magnetite. The distinction between high and low is meaningful only for each specimen and *not* for the whole Fiskensæset complex. Cr-free magnetites ( $Cr_2O_3 < 0.2$  wt. %) were texturally associated with sulphides thereby suggesting oxidation of the latter. The intimate textures of the Cr-bearing magnetite and ilmenite suggest oxidation of a Ti-bearing spinel to form ilmenite plus Cr-magnetite with low Ti. Further oxidation would cause conversion of some  $Fe^{2+} \rightarrow Fe^{3+}$  giving low-Cr magnetite and a Cr-rich magnetite. Undoubtedly many variations occur and the extent of reaction in any sample will vary. Whether the Ti-bearing spinel phase

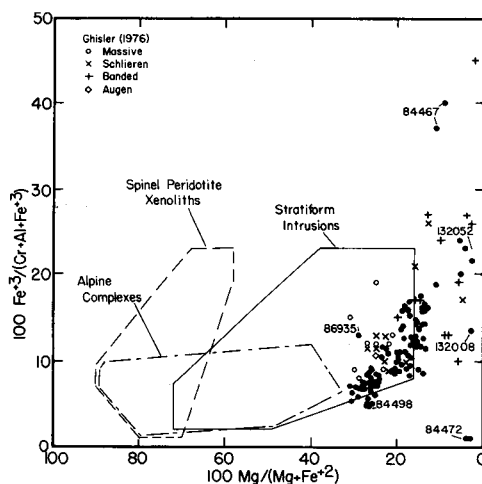


Fig. 5. As for fig. 33 except that  $cr$  is replaced by  $100 Fe^{3+}/(Fe^{3+} + Al + Cr)$ .  $Fe^{3+}$  was obtained by matching Ti by 2Fe, and splitting the remaining Fe into  $Fe^{2+}$  and  $Fe^{3+}$  to give 2:1 ratio of octahedral to tetrahedral cations.

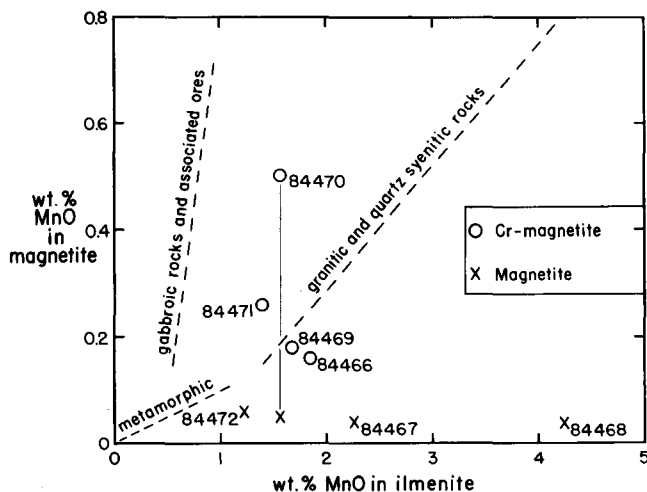


Fig. 6. Distribution of Mn between coexisting magnetite and ilmenite. The three lines show the trends found by Buddington & Lindsley (1964) for magnetite and titaniferous magnetite (1964, Fig. 12), and the data points show the Fiskensæset opaque oxides.

is primary is unknown, although some magnetite is clearly secondary during serpentinization.

#### Distribution of Mn between ilmenite and Cr-magnetite

Buddington & Lindsley (1964) summarized data on the distribution of Mn between ilmenite and titaniferous magnetite, and concluded that, with falling temperature of equilibration, the Mn showed increasing preference for the ilmenite (fig. 6). Ilmenite from the Fiskensæset samples coexists with Cr-bearing magnetite whose  $\text{Cr}_2\text{O}_3$  ranges from near zero to over 20%; some ilmenites coexist with more than one magnetite composition (see previous section). Data obtained by crystal spectrometer analysis for the Mn distribution (fig. 6) reveal that Cr-rich Cr-magnetite contains much more Mn than Cr-poor Cr-magnetite, best shown by 84470. Almost certainly the Mn distribution is not a simple indicator of the temperature of equilibration, and a correction for the Cr-content appears necessary. Considering just the Cr-poor Cr-magnetites whose compositions are closer to the specimens of Buddington & Lindsley, one might conclude tentatively that the Mn distribution in the Fiskensæset specimens results from a low temperature of equilibration. However, the specimens of Buddington & Lindsley contain much more Ti than those from Fiskensæset, and detailed deductions are unwise.

That ilmenite from specimen 84468 has by far the highest Mn content and the lowest ratio of Mn with respect to that in coexisting magnetite (with only 0.2 wt. %  $\text{Cr}_2\text{O}_3$ ) suggests a particularly low temperature of equilibration, which is consistent with almost total serpentinization of the olivine. Serpentine is also present in 84467 which shows the next highest MnO content in ilmenite. The Cr-magnetite rim in 84470 was interpreted in the previous section as the result of late-stage oxidation;

this specimen also shows serpentine and enrichment of Mn in ilmenite consistent with Cr-magnetite formation during serpentinization.

### Ti content of Cr-magnetite in relation to metamorphic grade

Buddington & Lindsley (1964, Fig. 2) showed that the Ti content of magnetite-ulvöspinel solid-solution coexisting with ilmenite decreased with temperature for each chosen buffered system. The fayalite-magnetite-quartz (FMQ) buffer probably gives conditions similar to those for the Fiskensæset assemblages. The Ti contents (crystal spectrometer data) of Cr-bearing magnetites coexisting with ilmenite in the Fiskensæset rocks (84466, TiO<sub>2</sub> 0.32 wt. %; 84467, 0.22; 84468, 0.18; 84469, 0.59; 84470, 0.21 in Cr-poor Cr-magnetite and 0.86 in Cr-rich Cr-magnetite; 84471, 0.81; 84472, 2.02) are much less than that found at 600°C by Buddington & Lindsley using the FMQ buffer. Extrapolation to lower temperatures indicates that these oxides in the Fiskensæset specimens equilibrated to temperatures well below 600°C, and perhaps as low as 300–400°C.

Textural study of all the above specimens revealed an excellent polygonal texture except for 84472 which has two unusual features: (1) deformed pyroxene megacrysts breaking down into subgrains and enclosing or being bordered by smaller grains, mostly of pyroxene and olivine, and (2) small scattered grains of biotite. The former indicates incomplete break-down of megacrysts into smaller grains with partial preservation of the original igneous texture of the silicates.

### Distribution of MnO, NiO, MgO and TiO<sub>2</sub> between coexisting oxides

Figs 7 and 8, respectively, show the distribution of MgO, NiO and MnO (crystal spectrometer data) between coexisting Cr-bearing magnetite and ilmenite, and of NiO, MnO and TiO<sub>2</sub> between coexisting Al-bearing magnetite or Cr-magnetite and spinel or Al-chromite.

Manganese strongly favours ilmenite over Cr-rich Cr-magnetite (Cr<sub>2</sub>O<sub>3</sub> > ~ 10 wt. %) and even more strongly over Cr-poor Cr-magnetite. Nickel favours the magnetites over the coexisting ilmenite, with no correlation with the Cr content of

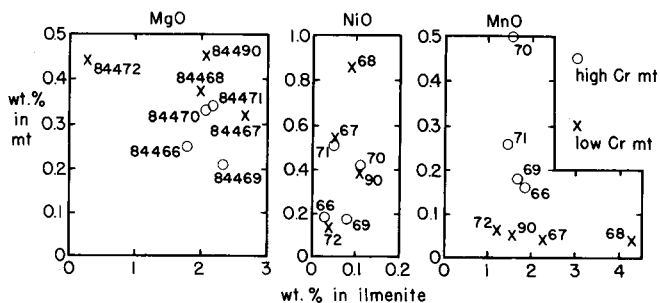


Fig. 7. Distribution of MgO, NiO and MnO between coexisting magnetite and ilmenite. The boundary between high- and low-Cr magnetites is at 10 wt. % Cr<sub>2</sub>O<sub>3</sub>.



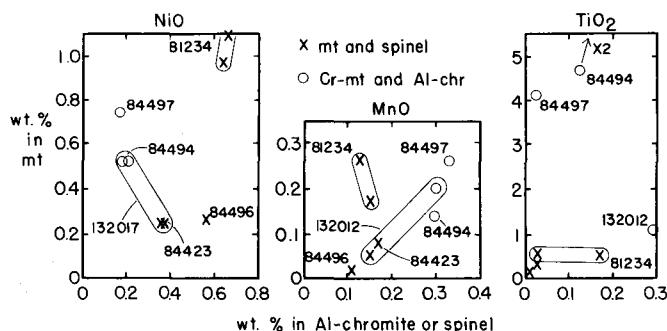


Fig. 8. Distribution of NiO, MnO and TiO<sub>2</sub> between coexisting magnetite and Al-chromite (see fig. 3).

the magnetites. Magnesium favours the ilmenite over coexisting Cr-magnetite, except for specimen 84472 (previously noted as unusual) in which the MgO content of the ilmenite is unusually low. The Mg content of Cr-rich Cr-magnetite is lower than for Cr-poor Cr-magnetite.

The distribution of NiO, MnO and TiO<sub>2</sub> between coexisting spinel-type phases is complex. Titanium always favours the magnetite-bearing phase regardless of Cr content although the high Cr content is associated with higher Ti content. Although higher MnO content is associated with higher Cr content, no preference is apparent between coexisting phases. Nickel is generally higher in Cr-poor coexisting phases, but shows no preference between coexisting phases.

The above trends are preliminary but the consistent distribution of some elements suggests an approach to equilibrium resulting from low-temperature metamorphism.

#### Primary chromites from zone Ch: comparison with other chromite data

Zone Ch chromites lie in the one phase field of fig. 3. Chemical data for two traverses across zone Ch are illustrated on fig. 9 as  $mg$  ( $= 100 \text{ Mg}/(\text{Mg} + \text{Fe})$ ) and  $fe^{+3}$  ( $= 100 \text{ Fe}^{+3}/(\text{Fe}^{+2} + \text{Fe}^{+3} + \text{Cr} + \text{Al})$ ). (To calculate the  $\text{Fe}^{+2}/\text{Fe}^{+3}$  ratio of the spinel, it was assumed that all Ti was tetravalent in the B site and coupled with  $\text{Fe}^{+2}$  in the A site; Mg, Ca, Mn and Ni were assumed divalent in the A site, and Al and Cr were assumed trivalent in the B site. The iron was then partitioned 1:2 in the A and B sites). Especially striking is the anticorrelation of these two variables for zone Ch a. Similar features occur for the upper samples in zone Ch b. Relations in the lower portion of zone Ch b are probably not reliable because some hand specimens did not contain chromite. However, mineral concentrates which sampled a larger volume did show chromite. Fig. 10 shows the oxide variations in chromite concentrates and the positive correlation of TiO<sub>2</sub>, Fe<sub>2</sub>O<sub>3</sub>, FeO, Cr<sub>2</sub>O<sub>3</sub> and MnO is apparent as is the positive correlation of Al<sub>2</sub>O<sub>3</sub> and MgO.

Although no consistent chemical trend from bottom to top is apparent in either traverse, one sample from each (132052 and 132037) is unusual in that the Fe<sub>3</sub>O<sub>4</sub>

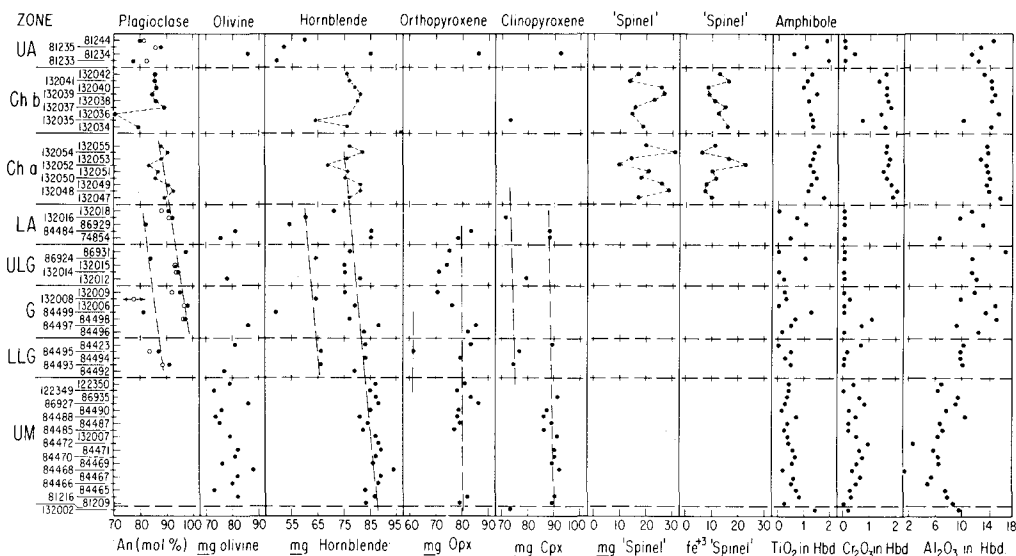


Fig. 9. Comparison of major chemical features of silicate and chromite-rich spinels plotted against stratigraphic position.

component (indicated by  $\text{Fe}_2\text{O}_3$ ) is considerably greater than for the other specimens. Windley & Smith (1974) also presented one analysis in their Ch c traverse which is unusual for its high  $\text{Fe}_3\text{O}_4$  content (132029). Because they were collected over a present-day distance of  $\sim 5$  km, it was not possible to correlate stratigraphically these specimens in the field. Perhaps they represent an unusual layer existing throughout a large part of the intrusion which might prove usable as a chemical

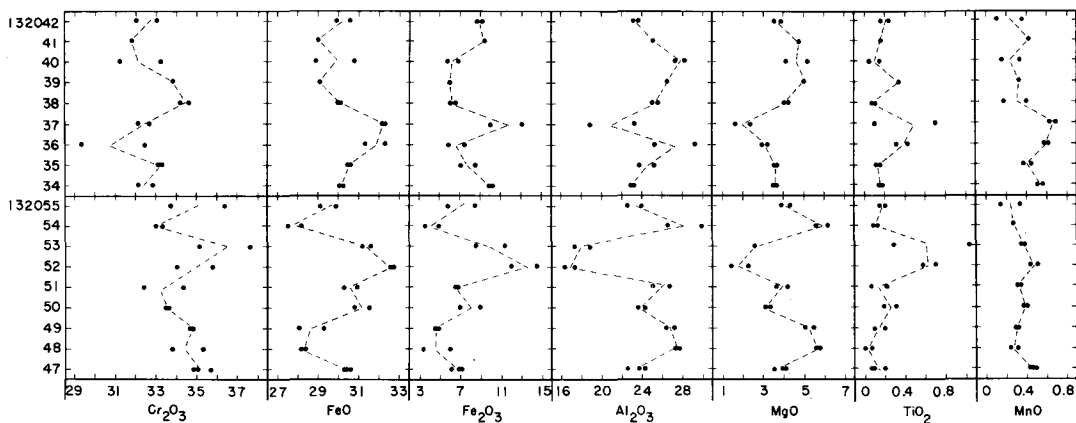


Fig. 10. Oxide variations in the two sequences from the Ch zone. Chromites from 132037 and 132052 are consistently different from other chromites in their respective zones. Data from mineral concentrates using wavelength spectrometer analysis.

marker for plotting detailed stratigraphy (note that silicate phases also show anomalous chemistry for these samples – see later).

The overall chemistry of the chromites is compared on figs 4 and 5 with generalized chromite data for other major layered intrusions (Bushveld, Great Dyke, Stillwater, Muskox) and chromite-bearing rocks (alpine intrusions and spinel peridotite xenoliths; Irvine, 1974a). As pointed out by Ghisler (1976), little or no overlap in chemistry is present. Basically, the Fiskensæset chromites are richer in Al than those of other layered intrusions and poorer in Mg than for alpine-type intrusions. The trivalent iron content (fig. 5) lies just within the range of layered intrusions.

### Origin of chromites (and other spinel types)

The presence of Al-rich chromites in zone Ch chromitites suggests a parent liquid more Al-rich than that inferred for other layered intrusions. This conclusion was also made by Windley *et al.* in Part I on the basis of whole-rock analyses and general chemical trends in the Fiskensæset complex. Experimental data for spinel crystallizing from a high-alumina basalt of lunar composition (Kushiro *et al.* 1972) show similar Al-rich compositions ( $\text{Cr}_2\text{O}_3$  20.0%,  $\text{Al}_2\text{O}_3$  48.5%, MgO 17.5%, FeO 13.5%) at pressures above 5 kb, but direct comparison is not possible because of the large difference in oxidation state for the experimental system and the postulated parent liquid of the Fiskensæset chromites. A more likely comparison is with terrestrial high-alumina basalts that are commonly associated with andesites in modern active Cordilleran margins. Chromite and chromian magnetite occur in the peridotites of the Duke Island complex, Alaska (Irvine, 1974a). Although Cr-spinel is absent in the Southern California batholith, Cr is concentrated in magnetite in the early gabbros (Simon & Rollinson, 1976) which Windley & Smith (1976) suggest may be a modern chemical analogue of the Fiskensæset complex.

The crystallization of the Fiskensæset chromites may be related to local conditions in the intrusion. Irvine (1974b) proposed that chromitites in the Muskox and Bushveld complexes and the Great Dyke formed when their magmas were contaminated by granitic melt derived by partial melting of overlying pelitic schist or granite during the sagging and breakage of the intrusion roof or during the influx of new magma along the roof. The following features of the Fiskensæset complex suggest that such a mechanism may have contributed to the precipitation of chromite.

(1) Sapphirine-bearing rocks commonly lie along the top interface of the complex (Herd *et al.*, 1969) where they are associated with marbles and mica schists. Whether they resulted from the metasomatic addition of granitic material to spinel-bearing ultramafic rocks (Herd *et al.*, 1969) or whether they represent metamorphic residua (restites) formed after extraction of anatectic granitic liquids from originally argillaceous sediments, as suggested for similar rocks by Clifford *et*

*al.* (1975), they provide key evidence of the generation of granitic melts along the intrusion roof.

(2) On eastern Manisat, just west of Qeqertarssuatsiaq, several metre-size rafts of marble lie against the zone Ch chromite seams, and in south central Qeqertarssuatsiaq there is a raft of quartz amphibolite about 30–60 cm across adjacent to a minor chromite-layered bronzitite near the boundary of zones LLG and G. Almost certainly these exotic inclusions were derived from the marbles and meta-volcanic quartz amphibolites that directly overlie the complex. Supracrustal inclusions are not known from other parts of the stratigraphic column. These relationships imply that roof material was dropping into the magma reservoir when the chromites were precipitating.

(3). Potassium is more abundant within and adjacent to the zone Ch chromitites than anywhere else in the intrusion, as is expressed by the common presence of biotite and lenses of garnet-biotite rock.

(4) Irvine (1974b) noted that MuskoX chromites contain various silicate inclusions together with some sulphides and rutile, the inclusions representing droplets of a contaminating granitic melt that was trapped in the crystallizing chromites. The Fiskeneset chromites of zone Ch abound in amphibole and rutile inclusions.

The origin of oxides parental to the present spinel-magnetite and Cr-magnetite–chromite intergrowths is more speculative because their bulk compositions are not accurately known. Detailed modal analysis of many grains or bulk analysis of carefully-separated material would be needed to give accurate data, and reaction with silicates may have changed the oxide compositions. Judging from routine optical study these intergrowths are usually dominated by the Al-rich component (81234 and 84423 are notable exceptions, but see later) and bulk compositions would plot close to the Al-rich limb of the solvus in fig. 3. Thus an origin of these spinel-type compositions from an Al-rich magma seems plausible.

Oxides on the magnetite-chromite join are compositionally and stratigraphically distinct from the aluminous varieties above. In a previous section, most present assemblages were inferred to result from oxidation of a Ti-bearing Cr-magnetite in addition to oxidation of sulphides and serpentinization. The appearance in the UM zone of silicates with numerous, small Cr-magnetite inclusions suggests the breakdown of silicates to some extent during oxidation. Whether all low-Al Cr-magnetite results from these processes is speculative, but the range of textures is not inconsistent with a sequence of processes in which at least some magnetite occurred initially as a dust in the ferromagnesian silicates: in many specimens the dust recrystallized at defects or took part in complete recrystallization yielding a polygonal texture with silicate grains. Perhaps detailed study may reveal some specimens which were sufficiently unaffected by the metamorphism to permit a clear test of the presence or otherwise of primary magnetite. Certainly the presence of appreciable amounts of Ti-rich oxide phases in association with the Cr-magnetite would be consistent with breakdown of a primary Ti-rich Cr-magnetite. The

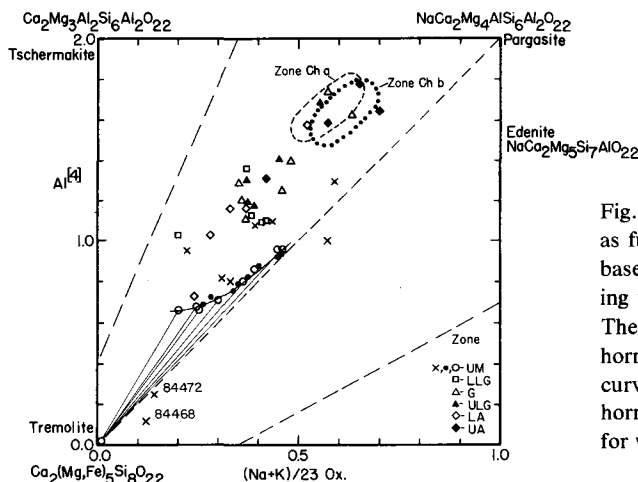


Fig. 11. Variation of amphibole composition as function of tetrahedral Al v. (Na + K) based on 23 oxygens. Tie lines join coexisting tremolite–hornblende in the UM zone. The compositions of the coexisting hornblende (open circles) fall on a smooth curve; solid circles indicate the UM zone hornblendes which fall along this curve but for which coexisting tremolite was not recognized.

question of the primary origin of the Cr-magnetite should be kept open at this time, but we shall assume in the conclusion that at least some Ti-rich Cr-magnetite was primary.

## CHEMISTRY OF SILICATES AND RELATION TO OXIDES

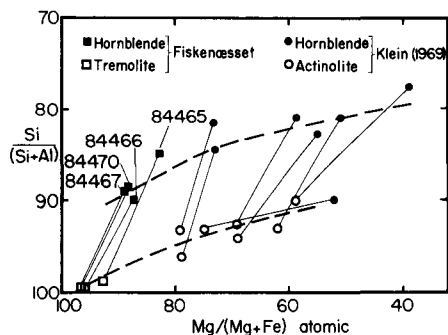
### Amphibole chemistry

Fig. 11 is a plot of tetrahedral Al against (Na + K) based on 23 oxygens. The range of compositions is almost identical to that given in Part II (Windley & Smith, 1974) except for new recognition of tremolite coexisting with hornblende in some specimens from the UM zone. Those hornblendes (open circles) which coexist with tremolite yield a monotonic curved trend on fig. 11. Other rocks whose hornblendes lie on this trend, but which apparently lack tremolite, might actually contain tremolite so far unrecognized. This would not be surprising because tremolite has very low abundance in all but one specimen, and diligent searching with an electron microprobe was necessary to obtain reliable identification of scattered tiny grains. Two rocks, 84472 and 84468, have hornblendes with compositions near the two-amphibole field, but differ from the other hornblendes in having  $2(\text{Na} + \text{K}) > \text{Al}^{\text{IV}}$ ; this subtle chemical difference may preclude growth of tremolite. Actinolite occurs in 84472.

Fig. 12 compares the coexisting amphiboles at Fiskensæset with actinolite–hornblende pairs attributed to the greenschist or amphibolite facies (Klein, 1969). On this plot of atomic  $\text{Mg}/(\text{Mg} + \text{Fe})$  v.  $\text{Si}/(\text{Si} + \text{Al})$ , Klein's trend is neatly extended to more Mg-rich compositions by the Fiskensæset data. Although there are no laboratory syntheses on the effect of temperature, pressure and bulk com-



Fig. 12. Variation of  $\text{Si}/(\text{Si} + \text{Al})$  v.  $\text{Mg}/(\text{Mg} + \text{Fe})$  for coexisting tremolite (or actinolite) and hornblende in the Fiskensæset complex compared to data for coexisting actinolite and hornblende in various other metamorphic rocks (Klein, 1969).



position on the coexistence of Ca-free and Ca-poor amphiboles, the similarity of the Fiskensæset ones with the metamorphic ones described by Klein is yet one more indication of the metamorphic grade of the Fiskensæset complex. Texturally the erratic spatial distribution of the Fiskensæset tremolite, and its close association to serpentine and minor unidentified phases with low oxide totals, indicates that it arises from a late metamorphic or metasomatic event in the greenschist facies. Anthophyllite occurs with actinolite in 84472.

### Pyroxene and olivine chemistry in relation to other minerals

The range of atomic  $\text{Mg}/(\text{Mg} + \text{Fe})$  for olivine is shown on fig. 9 as *mg* v. stratigraphic position. Nearly all zone UM rocks contain olivine, but it is sporadic in the LLG, G, ULG and LA zones. There is little change in *mg* olivine with zone although small changes (e.g. 84468) correlate with *mg* amphibole. Most obvious in a plot of *mg* olivine v. *mg* amphibole (fig. 13) is the separation of UM zone hornblendes from those in the LLG to LA zones, with considerable scatter in the latter. The reason for this is unknown, but may relate to presence of tremolite in the UM zone rocks. Springer's (1974) plot for a metamorphic ultrabasic complex in

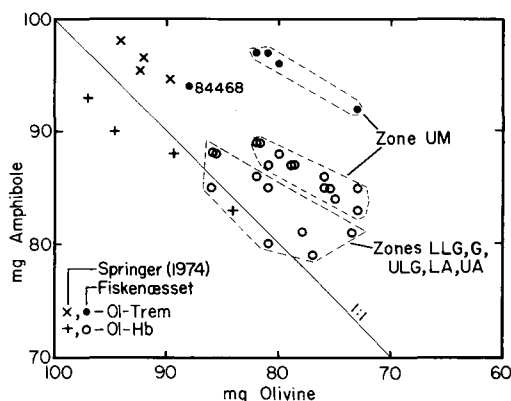


Fig. 13. Comparison of *mg* for coexisting amphibole and olivine. Springer's (1974) data for a meta-ultrabasic complex in California are also shown.

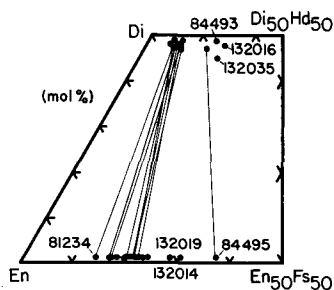


Fig. 14. Major-element composition of Fiskensæset pyroxenes shown on part of the En–Di–Hd–Fs quadrilateral. Rock numbers are given for pyroxenes which deviate from the main concentration.

California shows Mg enriched in the amphibole phase relative to olivine to a greater extent than for most Fiskensæset pairs. These changes in *mg* partition probably result from variation in bulk composition of the amphibole, but there are no systematic laboratory studies to provide a reliable test.

The ranges of pyroxene compositions (fig. 14) are similar to those given in Part II. Most clinopyroxenes (fig. 9) have *mg* near 90, perhaps with a slight trend to lower *mg* with increasing stratigraphic height, but six have *mg* between 70 and 80; of course, many more specimens from across the Fiskensæset complex are needed to check whether the dashed lines in fig. 9 represent two distinct trends. Most orthopyroxenes have *mg* between 70 and 85, but one is distinctly more Fe-rich with *mg* 61. That the rocks with Fe-rich pyroxenes also have Fe-rich amphiboles and Na-rich plagioclases suggests that some general feature is responsible for the unusual mineral compositions, but no definitive explanation is currently available; perhaps the composition variations result from cryptic layering throughout the whole complex. Note from fig. 9 that there is a stronger variation of *mg* with stratigraphic position for the main *mg*-rich group of amphiboles than for the main *mg*-rich groups of pyroxenes.

### Plagioclase chemistry

The general trend of Na enrichment with higher stratigraphic position (fig. 9) is similar to that reported in Part II, but seven rocks from the LLG to LA zones have distinctly more sodic plagioclases than nearby rocks. Windley & Smith (Part II) had already noted this feature, but their suggestion that it correlates with the presence of chromite is now seen to be wrong on the basis of the present larger suite. As mentioned in the preceding section, the Na-rich plagioclases coexist with the Fe-rich ferromagnesian silicates.

### Silicate–oxide relations

Fig. 9 shows that *mg* (hornblende) correlates closely with *mg* and *fe*<sup>+3</sup> of chromite in the Ch zone. The Cr<sub>2</sub>O<sub>3</sub> content of hornblende ranges from near zero in

the ULG and LA zones to values mostly between 1.5 and 2 wt. % in chromitites from the Ch zone. In the lower zones, the  $\text{Cr}_2\text{O}_3$  values range erratically from 0 to 1 wt. %. Much further study is needed to determine the factors which control the Cr content of the hornblende; probably the bulk composition of the host rock is determined by mechanical accumulation of crystals during igneous fractionation (thus the Cr content would be very high for chromitites), and the partition of Cr is determined by the types of minerals participating in the subsequent metamorphic equilibration.

There is no apparent correlation between the Ti content of amphibole (fig. 9) and the occurrence of rutile and ilmenite (table 1). All amphiboles from the chromitites of the Ch zone have high Ti contents, and amphiboles from the rocks with Fe- and Na-rich minerals (fig. 9) also tend to have high Ti. Aluminium is high in amphiboles from the Ch zone chromitites, but varies greatly for other specimens with an overall tendency to increase with stratigraphic height.

The An content of plagioclase decreases as *mg* decreases and *fe*<sup>+3</sup> increases in the chromite, as is particularly well displayed in zone Ch a (fig. 9).

## GEOOTHERMOMETRY USING TWO PYROXENES AND OXIDE-SILICATE

### Two pyroxenes

The diopside–enstatite miscibility gap varies with temperature, is almost independent of pressure, and is affected by substitution of elements for Mg, Ca and Si. Unfortunately there is considerable discrepancy between the experimental data obtained in different laboratories for the pure En–Di system (e.g. Davis & Boyd, 1966; Nehru & Wyllie, 1974; Mori & Green, 1975) and data were not available below 950°C. As a temporary expedient, we used the calculation procedure of Wood & Banno (1973) which takes into account compositional divergence from the En–Di join and which allows extrapolation below 950°C.

Table 5 gives temperatures ranging from 830 to 890°C for 11 clinopyroxenes coexisting with orthopyroxene in ultramafic layers from the UM zone and ultramafic lenses in the LLG, LA and UA zones. These estimated temperatures show no trend with zone, and the range of 60°C could be attributed merely to analytical error. Hence one could conclude that the entire suite of samples was subjected to essentially the same metamorphic conditions. The Wood-Banno procedure is based essentially on the data of Davis & Boyd. Perhaps the data of Nehru & Wyllie might be preferred because they used an electron microprobe to analyze the composition of the coexisting pyroxenes rather than using X-ray powder data; if so, one might prefer to lower the mean temperature of ~860°C from the Wood-

*Table 5. Estimates of temperature for mineralogical equilibration*

(a) Two-pyroxene thermometer: Wood-Banno model		
Sample	Zone	Temperature (°C)
81234	UA	840
84484	LA	860
74854	LA	890
84423	LLG	890
86935	UM	880
84490	UM	830
84488	UM	890
84487	UM	860
84485	UM	880
81216	UM	840
81209	UM	830

(b) Ilmenite-silicate thermometer: Bishop model					
Sample	Zone	Temperature(°C)			
		olivine	clinopyroxene	orthopyroxene	'mean'
84484	LA	690	760	740	730
74854	LA	610	660	650	640
84497	G	630	-	710	670
122350	UM	650	-	690	670
122349	UM	680	-	690	690
84490	UM	650	700	700	680
84488	UM	650	680	690	680
84487	UM	680	700	720	700
84485	UM	-	650	660	650
132007	UM	600	650	-	630
84471	UM	560	650	-	600
84470	UM	570	650	-	610
84469	UM	580	610	-	600
84468	UM	480	660	-	570
84467	UM	580	-	-	580
84466	UM	670	-	-	670
81216	UM	660	730	720	700

Temperatures rounded to nearest 10°C.

Banno procedure to about 700°C for the extrapolation of the Nehru-Wyllie data. Unfortunately reactions are very sluggish below 1000°C and controversy on the position of the diopside–enstatite solvus is likely to continue. (New data by Lindsley & Dixon (1976) further emphasize the problems of determining the equilibrium solvus at low temperatures).

### Ilmenite–silicate and chromite–amphibole

Anderson *et al.* (1972) predicted from fragmentary data that the distributions of  $\text{Fe}^{2+}$  and  $\text{Mg}^{2+}$  between ilmenite and pyroxenes should be strongly sensitive to temperature. This was confirmed by Bishop (1976) from controlled syntheses of ilmenite, pyroxenes and also olivine. Fortunately the distributions are only slightly sensitive to pressure, and the estimated temperatures for Fiskensæset specimens (table 5) would change by less than 10°C if the assumed pressure of 7 kb were wrong by 1 kb. Analytical error in the electron microprobe analyses could give an error of at least  $\pm 30^\circ\text{C}$  ( $1\sigma$ ), especially for the very fine inclusions of ilmenite in a magnetite host. The different temperatures for the same rock can probably be ascribed to analytical error rather than to a genuine difference of equilibrium temperature between mineral pairs (except perhaps for 84468).

The mean temperatures in table 5 for ultramafic layers in zone UM and lenses in zones G and LA show erratic variations in the range 580–730°C with no indication of a zonal trend, thereby confirming the conclusion from the pyroxene thermometer. The ilmenite–silicate temperatures tend to be  $\sim 200^\circ\text{C}$  lower than the Wood-Banno pyroxene temperatures and  $\sim 100^\circ\text{C}$  lower than the Nehru-Wyllie ones. One tremolite-bearing specimen has a low ilmenite–silicate temperature (84468) which is consistent with the earlier suggestion that equilibration took place to a metamorphic grade lower than for the main bulk of the complex. Specimen 81209 was not used to derive a temperature because of uncertainty of identification of ilmenite; the high Mn and Cr content, and the deviation from the 2:3 metal/oxide ratio (table 3), suggest that the electron microprobe analyses of the very tiny grains do not represent a pure ilmenite.

Although there are no systematic experimental data on the partition of Mg/Fe between chromite and hornblende, crystal-chemical arguments strongly imply that it should have a similar temperature dependency to the partition for ilmenite and pyroxene. If so, with falling temperature, Mg should migrate out of the chromite into the hornblende. Although our specimens showed essentially no compositional difference between poikilitic and clean chromite, those of Ghisler (1976) showed distinctly lower Mg in the clean than in the poikilitic chromite. Thus Ghisler's data can be explained by the poikilitic chromite having equilibrated with hornblende (and other Fe, Mg-silicates) at a higher temperature than the clean chromite. Apparently the recrystallization of the poikilitic chromite to the clean chromite was not followed by metamorphic equilibration of the entire chromite cluster in

Ghisler's specimens in contrast to our specimens. Complete equilibration over an entire thin section did not occur in all our specimens, as shown by the different analyses for 2 grains in 132050 (table 4).

## GENERAL DISCUSSION AND CONCLUSIONS

The present data support the earlier interpretation of the Fiskensæset complex as a metamorphosed igneous complex derived from a moderately wet Al-rich basaltic magma undergoing crystal-liquid differentiation under fairly oxidizing conditions. Important mineralogical and petrological features were reviewed by Windley & Smith (1976). The original igneous assemblage apparently involved early precipitation of Mg-Al-Ti-Cr-magnetite, prolonged crystallization of highly calcic plagioclase and tschermakitic-magnesio-hornblende, and late crystallization of high-Fe, medium-Cr spinel. Most of the original minerals have been transformed by complex sub-solidus reactions, and the present mineral assemblages have equilibrated to different temperatures which depend on the ease of migration of components and the local metamorphic level. The present study has used optical microscopy and electron microprobe analyses with a spatial resolution near 1  $\mu\text{m}$ . Use of spectral and diffraction techniques should reveal movements down to the atomic level, and after further instrumental development the ion microprobe should reveal the fine-scale spatial distribution of trace elements and isotopes. But these studies remain for the future delectation of research mineralogists, and in the meantime we pull together the information applying to metamorphic equilibration on the scale of 1  $\mu\text{m}$  or greater. Of course, one must always bear in mind that (a) the bulk composition is determined by the mechanical and chemical aspects of the original igneous differentiation, provided that metasomatism has not occurred, and that (b) caution is needed in deducing the spatial extent of metamorphic equilibration from textural observations.

With these caveats, we conclude that the oxide assemblages result mostly from the transformation of single-phase Ti-Cr-Al-magnetite (especially prominent in the lower zones) and Fe,Cr-rich spinel (loosely called chromite, and especially prominent in the Ch zone). Because the partition of Mg and Fe (and presumably other elements as well) between oxide and silicate depends on temperature, the present bulk composition of oxide assemblages is not that of the igneous precursors. Using the ilmenite-silicate assemblage as an analogy for the chromite-silicate assemblage, one can conclude that the present metamorphic chromites are less magnesian than their igneous precursors (preceding section). Referring to figs 4 and 5, it will be seen that increasing the Mg content of the chromites would move them towards the range for dry basaltic stratiform complexes. Highly desirable are controlled heating experiments of chromite-rich rocks from the Fiskensæset complex to determine the

extent of element migration from chromite to silicate when the temperature is raised to the solidus. It is impossible from the present data to determine accurately the change of composition produced by metamorphic equilibration, but because there is no systematic major change of chromite composition with ratio of chromite to silicate minerals (e.g. compare the chromite compositions for gabbro 132008 and ultramafic rocks 84467 and 84472 in fig. 4), we conclude that the primary chromites probably were richer in Fe than those from dry basaltic stratiform complexes. Furthermore, those at Fiskenæsset appeared late in the stratigraphic column whereas those from the dry basaltic complexes appeared early. Presumably the assemblages rich in Cr-magnetite at Fiskenæsset have also undergone some element exchange with the silicates, and they certainly have been modified in some rocks by exsolution of Cr-magnetite from the Fe, Mg-silicates. Nevertheless, the high concentration of Cr-magnetite in some ultramafic rocks is most easily interpreted in terms of a primary igneous origin, especially as this provides a partial explanation for the near lack of iron enrichment at Fiskenæsset in contrast to that for dry basaltic intrusions such as the Skaergaard complex.

Several estimates of the temperature of metamorphic equilibration were presented in earlier sections. The scattered occurrences of serpentine, tremolite and biotite are best interpreted as the result of erratic local metasomatism in the greenschist facies, at least for the first two minerals. The bulk of the complex, however, appears to have retained or nearly retained the original igneous bulk composition except perhaps for partial conversion of pyroxenes to hornblende. If the temperature estimates given in earlier sections are valid, the pyroxenes would have ceased to equilibrate at a higher temperature (perhaps  $\sim 700\text{--}800^\circ\text{C}$ ) than ilmenite and Fe, Mg-silicates (perhaps mostly  $\sim 600\text{--}700^\circ\text{C}$ ), but the possibility of revised laboratory calibrations must be borne in mind. Such equilibrations involve element migration over the typical grain size of about 0.5 mm. Experimental calibrations for the coexisting oxides are particularly poor, but those for coexisting spinel minerals suggest a temperature well below  $600^\circ\text{C}$ ; here the scale for migration is often less than 0.1 mm, but some of the 'shadow' zones are considerably wider than 0.1 mm. In Part IV, data for the coexisting sulphides will be found to indicate equilibration down to  $100\text{--}200^\circ\text{C}$ . Thus no simple statement is possible about the metamorphic conditions, and each rock, each grain, and each assemblage must be examined in terms of its tectonic environment, its mineral types, and the quality of the relevant experimental calibrations. In classical terms, the very crude statement could be made that most of the Fiskenæsset complex has retrogressed from the granulite into the amphibolite facies with local excursion into the greenschist grade.

For the spinels, recognition of the 2-phase region provides an opportunity for development of a geothermometer by careful experimental syntheses. Our data for relatively few hand specimens actually show a greater range of spinel group compositions than those found by Ghisler for a much larger suite of specimens, and

even greater variation might be expected when the whole complex is studied. The data in fig. 4 show that most chromites (*sensu lato*) from the Fiskenæsset complex are more aluminous than those from dry basaltic stratiform complexes. Probably this general feature does not result from metamorphic equilibration with the silicates, though small changes should occur in the Al/Cr ratio of the chromites from this process (cf. Ghisler, 1976). Furthermore the aluminous nature of the chromites would correlate with the aluminous bulk composition of the overall complex.

Numerous speculations of a mineralogical and geochemical nature could be made about the oxide and silicate minerals in the Fiskenæsset complex (e.g. does a wet basaltic magma tend to retain  $\text{Cr}^{2+}$  ions because of interaction with hydroxyl anions?), but we merely conclude by pointing out the remarkable opportunities for further studies especially of sub-microscopic textures and relevant phase equilibria.

### Acknowledgements

We thank the Director of the Geological Survey of Greenland for field facilities in Greenland. Dr. A. T. Anderson kindly discussed various aspects of oxide equilibria. Helpful comments from M. Ghisler, R. Phillips and S. Watt were used in revision of the manuscript. Financial support came from National Science Foundation grants GA-21132 and EAR76-03604, National Aeronautics and Space Administration grant 14-011-171, and grant GR3/1758 from the Natural Environment Research Council. F. C. Bishop thanks NSF for a Graduate Fellowship. Electron microprobe analyses were partly supported by the Materials Research Laboratory funded by NSF. We thank I. Baltuska, O. Draughn, P. Matkovits and T. Solberg for technical help. This paper is a contribution to the International Geological Correlation Project on Archaen Geochemistry.

## APPENDIX

### Petrographic notes on analyzed samples

#### Zone UA

- 81244 Anorthosite. Greenish-brown hornblende. Large garnets have inclusions of plagioclase and hornblende.
- 81235 Anorthosite. A few green hornblendes interspersed within a polygonal mosaic of plagioclase. Rare ilmenite. Opaque grains essentially lacking.
- 81234 Ultramafic. Olivine, orthopyroxene and green hornblende form a granular fabric of nearly equidimensional grains in roughly equal proportions. Common magnetite-spinel granules lie mostly along silicate grain boundaries. All chromite-bearing samples from zone Ch are essentially similar. The chromite occurs with only minor plagioclase in hornblende-rich areas; these form a web around ellipsoidal areas of polygonal plagioclase which are interpreted as recrystallized plagioclase megacrysts. Plagioclases show a strong tendency towards planar grain boundaries and equilibrium triple junctions. Chromites are sub-idiomorphic, often packed together in dense clusters or linked to each other. Rutile occurs within chromites or adjacent to them.
- 81233 Hornblende anorthosite. Polygonal plagioclase network with a few greenish-brown hornblendes situated at plagioclase junctions.



*Zone Ch*  
*Chromitites*

132037 and 132052 Chromitites. These have about 50% and 5% biotite respectively.

132036 and 132052 Chromitites. Epidote and muscovite developed from hornblende and plagioclase. All other chromitites are fresh and unaltered. The amount of chromite varies considerably between 7% and 67% as follows:

	vol. %		vol. %		vol. %
132055	25	132049	32	132039	49
132054	35	132048	17	132038	25
132053	8	132047	14	132037	67
132052	8	132042	7	132036	35
132051	19	132041	24	132035	15
132050	17	132040	21	132034	62

*Zone LA*

132018 Hornblende anorthosite. Some green hornblende with coarse polygonal plagioclase mosaic. No opaque grains.

132016 Anorthosite. As above but with very rare green hornblende and clinopyroxene.

86929 Leucogabbro. Plagioclase mosaic intergrown with brown hornblende. Rare opaque grains.

84484 Peridotite. Granular mosaic of roughly equidimensional green hornblende, orthopyroxene and clinopyroxene and olivine. Common green spinel and opaque oxides and sulphides scattered through the rock, often at silicate boundaries.

74854 Hornblende peridotite. Much green hornblende with clinopyroxene, orthopyroxene and olivine. Abundant opaque granules within and between silicates.

*Zone ULG*

86931 As 132014 plus a little orthopyroxene and rare opaque grains.

86924 Leucogabbro. Plagioclase – green hornblende intergrowth. Rare opaque grains.

132015 Gabbro. Semi-polygonal mosaic of pale green hornblende and plagioclase and a few small orthopyroxenes. No opaque grains.

132014 Leucogabbro with polygonal plagioclase intergrown with coarse green hornblende. No opaque grains.

132012 Ultramafic. Olivine, orthopyroxene and hornblende are intergrown in a granular fabric of equant grains. Abundant green spinel and less common chromite are confined to hornblende areas occurring largely along hornblende grain boundaries; these define an oxide layering in the rock.

*Zone G*

132009 Hypersthene gabbro. Green hornblende–plagioclase network plus small to large pink orthopyroxenes. Some large plagioclase grains contain abundant hornblende micro-needles. No opaque grains.

132008 Leucogabbro. Coarse plagioclase – green hornblende intergrowth. Rare scattered grains of clinopyroxene and biotite. Rare opaque grains.

132006 Gabbro with lineated coarse green hornblende and fine-grained plagioclase with interspersed lineated granules of orthopyroxene. Rare opaque grains.

84498 Gabbro. Chromite (only a few percent) occurs as isolated subidiomorphic grains within hornblende and defines a chromite layering. Polygonal plagioclases occur in thin layers between and among hornblende-chromite layers.

- 84497 Ultramafic. Chromite forms well-defined seams within hornblende-rich layers separated by orthopyroxene-olivine-rich layers.
- 84496 Hornblende-orthopyroxene rock with a dense concentration of opaque oxides mostly within the orthopyroxene. Fine-grained opaque oxide dust is concentrated within the cores of larger orthopyroxenes. Larger opaque grains occur in the border zones, in smaller orthopyroxenes, and in hornblendes.

#### *Zone LLG*

- 84423 Peridotite. Weakly oriented network of olivine, green hornblende, clinopyroxene and orthopyroxene. Common green spinel and opaque grains.
- 84495 Leucogabbro. Polygonal plagioclase network with interspersed green hornblende and clinopyroxene.
- 84494 Ultramafic. Granular grains of hornblende and orthopyroxene form interlocking equilibrium fabric. Opaque oxides (including green spinel, not analysed) define a weak layering parallel to the long direction of the amphiboles.
- 84493 Leucogabbro with weakly aligned plagioclase and green hornblende. A little scattered clinopyroxene.
- 84492 Hornblende peridotite consisting of a roughly equidimensional network of green hornblende, olivine and pink orthopyroxene. Abundant opaque grains along silicate grain boundaries.

#### *Zone UM*

- 122350 Ultramafic. An oriented fine-grained granular mosaic of pale yellow-brown hornblende, olivine and orthopyroxene. Abundant opaque grains.
- 122349 Ultramafic. Within a fine-grained unoriented granular mosaic of pale yellow-brown hornblendes and olivines there are scattered skeletal megacrysts of olivine and orthopyroxene. Common opaque phases occur within the megacrysts and along matrix grain boundaries.
- 86935 Chromite-layered ultramafic. Layers rich in clinopyroxene and orthopyroxene, and containing minor hornblende, alternate with layers rich in chromite and green hornblende.
- 86927 Ultramafic. Granular mosaic of green hornblende, pink orthopyroxene and olivine contains abundant subidiomorphic large oxide grains mostly concentrated in layers throughout the silicate matrix.
- 84490 Peridotite. Intergrowth of green hornblende, olivine, clinopyroxene and orthopyroxene. Opaque grains common.
- 84488 Peridotite. Green hornblende, orthopyroxene, olivine and coarse clinopyroxene intergrown mostly in a granular network. Some orthopyroxenes, hornblendes and clinopyroxenes have cores sieved with abundant opaque oxide dust. Opaque granules also scattered through the rock.
- 84487 Peridotite. Very regular granular intergrowth of equidimensional green hornblende, clinopyroxene, orthopyroxene and olivine. Common opaque granules mostly at silicate boundaries.
- 84485 Ultramafic. Abundant green hornblende interlocked with a little clinopyroxene and orthopyroxene. Abundant opaque grains including fine dust within some hornblende grains.
- 132007 Peridotite with olivine, green hornblende and minor clinopyroxene. A few accessory opaque grains.
- 84472 Ultramafic. Two pyroxenes and colourless to faint brown hornblende are the main constituents with uncommon biotite and rare quartz. Opaque oxides are rare.
- 84471 Ultramafic. Faint brown hornblende, two pyroxenes and rare olivine are mutually intergrown to form a granular texture with frequent isolated granules of magnetite homogeneously distributed throughout the rock.

- 84470 Ultramafic. A granular mosaic of interlocking olivine and hornblende (pale brown) grains with widely scattered, isolated magnetite granules. The rock is traversed by cracks filled with serpentine which has a central zone of magnetite.
- 84469 Ultramafic. A nearly perfect equilibrium fabric of interlocking equant grains of olivine and hornblende (pale brown) with common triple junctions between these minerals. Scattered magnetite granules occur within both minerals rather than along grain boundaries.
- 84468 Serpentinized hornblende dunite. Boundaries of many original olivines are outlined by magnetite. Magnetite occurs as seams and granules within serpentine and as granules within hornblende.
- 84467 Hornblende-diopside peridotite traversed by abundant seams of serpentine often with central zones of magnetite. Magnetite also occurs as individual subidiomorphic grains within olivine.
- 84466 Ultramafic. Equilibrium texture of polygonal olivine and hornblende (pale brown) grains with planar boundaries and triple junctions. Isolated common magnetite grains have a strong affinity for olivine.
- 84465 Hornblende-olivine rock. Tremolite occurs as fine-grained polycrystalline areas in which dark grains outline an original coarse polygonal texture. Abundant magnetite grains are scattered homogeneously through the rock.
- 81216 Ultramafic. Granular mosaic of olivine, brown hornblende, clinopyroxene and orthopyroxene. Opaque granules common.
- 81209 Ultramafic. Predominant deep-green, coarse hornblende and minor smaller grains of orthopyroxene and clinopyroxene. Common oxide and sulphide granules along silicate grain boundaries.

## REFERENCES

- Anderson, A. T., Braziunas, T. F., Jacoby, J. & Smith, J. V. 1972: Thermal and mechanical history of breccias 14306, 14063, 14270, and 14321. *Geochim. cosmochim. Acta Suppl.* **3**, 1, 819–835.
- Bishop, F. C. 1976: *Partitioning of Fe<sup>2+</sup> and Mg between ilmenite and some ferromagnesian silicates*. Ph. D. thesis, University of Chicago.
- Black, L. P., Moorbath, S., Pankhurst, R. J. & Windley, B. F. 1973: The <sup>204</sup>Pb/<sup>206</sup>Pb whole rock age of the Archaean granulite facies metamorphic event in West Greenland. *Nature Phys. Sci.* **244**, 50–53.
- Buddington, A. F. & Lindsley, D. H. 1964: Iron-titanium oxide minerals and synthetic equivalents. *J. Petrol.* **5**, 310–357.
- Clifford, T. N., Stumpfl, E. F. & McIver, J. R. 1975: A sapphirine-cordierite-bronzite-phlogopite paragenesis from Namaqualand, South Africa. *Mineralog. Mag.* **40**, 347–356.
- Cremer, V. 1966: *Die Mischkristallbildung im System Chromit-Magnetit-Hercynit zwischen 1000°C und 500°C*. Diss. Univ. München, 44 pp.
- Cremer, V. 1969: Die Mischkristallbildung im System Chromit-Magnetit-Hercynit zwischen 1000°C und 500°C. *Neues Jb. Miner. Abh.* **111**, 184–205.
- Davis, B. T. C. & Boyd, F. R. 1966: The join Mg<sub>2</sub>Si<sub>2</sub>O<sub>6</sub>-CaMgSi<sub>2</sub>O<sub>6</sub> at 30 kilobars pressure and its application to pyroxene from kimberlites. *J. geophys. Res.* **71**, 3567–3576.
- Ghisler, M. 1970: Pre-metamorphic folded chromite deposits of stratiform type in the early Precambrian of West Greenland. *Mineral. Deposita* **5**, 223–236.
- Ghisler, M. 1976: The geology, mineralogy and geochemistry of the pre-orogenic Archaean stratiform chromite deposits at Fiskensæset, West Greenland. *Monogr. Series Mineral Deposits* **14**, 156 pp.
- Ghisler, M. & Windley, B. F. 1967: The chromite deposits of the Fiskensæset region, West Greenland. *Rapp. Grønlands geol. Unders.* **12**, 38 pp.
- Henderson, P., Fishlock, S. J., Laul, J. C., Cooper, T. D., Conrad, R. L., Boynton, W. V. & Schmitt,

- R. A. 1976: Rare earth element abundances in rocks and minerals from the Fiskenæsset complex, West Greenland. *Earth Planet. Sci. Lett.* **30**, 37–49.
- Herd, R. K., Windley, B. F. & Ghisler, M. 1969: The mode of occurrence and petrogenesis of the sapphirine-bearing and associated rocks of West Greenland. *Rapp. Grønlands geol. Unders.* **24**, 44 pp.
- Irvine, T. N. 1974a: Petrology of the Duke Island ultramafic complex, southeastern Alaska. *Mem. geol. Soc. Am.* **138**, 240 pp.
- Irvine, T. N. 1974b: Chromitite layers in stratiform intrusions. *Yb. Carnegie Instn Wash.* **73**, 300–316.
- Klein, C. Jr. 1969: Two-amphibole assemblages in the system actinolite-hornblende-glaucophane. *Amer. Mineral.* **54**, 212–237.
- Kushiro, I., Ikeda, Y. & Nakamura, Y. 1972: Petrology of Apollo 14 high-alumina basalt. *Geochim. cosmochim. Acta Suppl.* **3**, **1**, 115–129.
- Lindsley, D. H. & Dixon, S. A. 1976: Diopside-enstatite equilibria at 850° to 1400°C, 5 to 35 kb. *Amer. J. Sci.* **276**, 1285–1301.
- Morgan, J. W., Ganapathy, R., Higuchi, H. & Krähenbühl, U. 1976: Volatile and siderophile trace elements in anorthositic rocks from Fiskenæsset, West Greenland: comparison with lunar and meteoritic analogues. *Geochim. cosmochim. Acta* **40**, 861–887.
- Mori, T. & Green, D. H. 1975: Pyroxenes in the system  $Mg_2Si_2O_6$ – $CaMgSi_2O_6$  at high pressure. *Earth Planet. Sci. Lett.* **26**, 277–286.
- Muir, J. E. & Naldrett, A. J. 1973: A natural occurrence of two-phase chromium-bearing spinels. *Can. Miner.* **11**, 930–939.
- Myers, J. S. 1975: Igneous stratigraphy of Archaean anorthosite at Majorqap qáva, near Fiskenæsset, South-West Greenland. *Rapp. Grønlands geol. Unders.* **74**, 27 pp.
- Myers, J. S. 1976a: Channel deposits of peridotite, gabbro and chromitite from turbidity currents in the stratiform Fiskenæsset anorthosite complex, southwest Greenland. *Lithos* **9**, 281–291.
- Myers, J. S. 1976b: Granitoid sheets, thrusting, and Archean crustal thickening in West Greenland. *Geology* **4**, 265–268.
- Myers, J. S. & Platt, R. G. 1977: Mineral chemistry of layered Archaean anorthosite at Majorqap qáva, near Fiskenæsset, southwest Greenland. *Lithos* **10**, 59–72.
- Nehru, C. E. & Wyllie, P. J. 1974: Electron microprobe measurements of pyroxenes coexisting with  $H_2O$ -undersaturated liquid in the join  $CaMgSi_2O_6$ – $Mg_2Si_2O_6$ – $H_2O$  at 30 kilobars, with applications to geothermometry. *Contr. Mineral. Petrol.* **48**, 221–228.
- Rucklidge, J. 1967: A computer program for processing microprobe data. *J. Geol.* **75**, 126.
- Simon, F. O. & Rollinson, C. L. 1976: Chromium in rocks and minerals from the Southern Californian batholith. *Chem. Geol.* **17**, 73–88.
- Springer, R. K. 1974: Contact metamorphosed ultramafic rocks in the western Sierra Nevada foothills, California. *J. Petrol.* **15**, 160–195.
- Sweatman, T. R. & Long, J. V. P. 1969: Quantitative electron-probe microanalysis of rock-forming minerals. *J. Petrol.* **10**, 332–379.
- Turnock, A. C. & Eugster, H. P. 1962: Fe-Al oxides: phase relationships below 1000°C. *J. Petrol.* **3**, 533–565.
- Windley, B. F., Herd, R. K. & Bowden, A. A. 1973: The Fiskenæsset complex, West Greenland, Part I. A preliminary study of the stratigraphy, petrology and whole rock chemistry from Qeqertarsuatsiaq. *Bull. Grønlands geol. Unders.* **106** (also *Meddr Grønland* **196**, 2), 80 pp.
- Windley, B. F. & Smith, J. V. 1974: The Fiskenæsset complex, West Greenland, Part II. General mineral chemistry from Qeqertarsuatsiaq. *Bull. Grønlands geol. Unders.* **108** (also *Meddr Grønland* **196**, 4), 54 pp.
- Windley, B. F. & Smith, J. V. 1976: Archaean high grade complexes and modern continental margins. *Nature* **260**, 671–675.
- Wood, B. J. & Banno, S. 1973: Garnet-orthopyroxene and orthopyroxene-clinopyroxene relationships in simple and complex systems. *Contr. Mineral. Petrol.* **42**, 109–124.

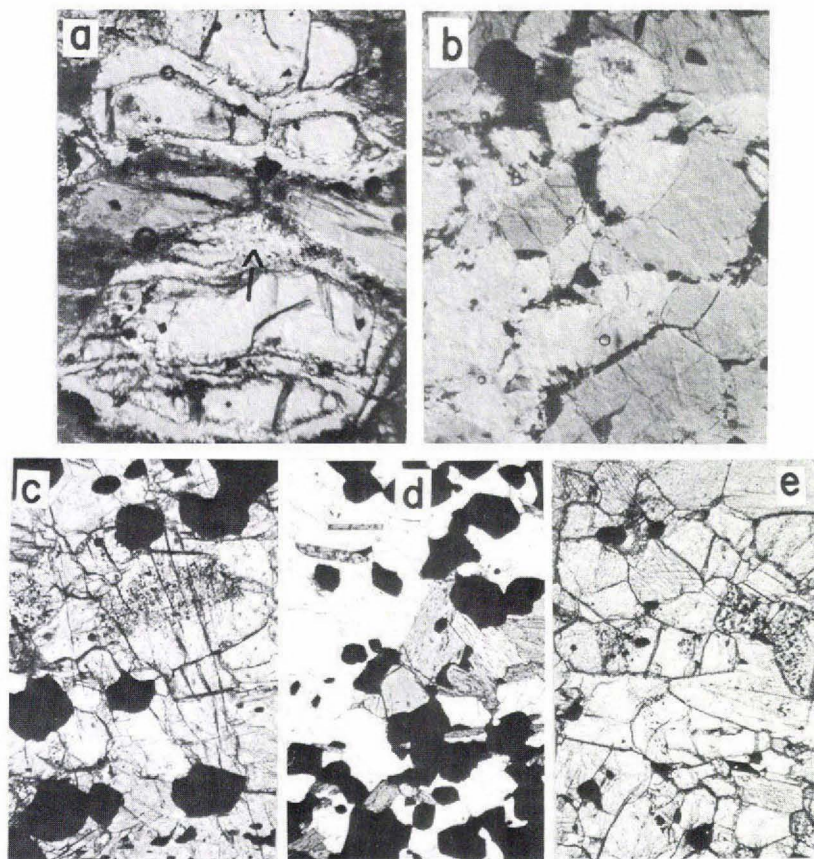


### Plate 1

- a: Marginal alteration of olivine (clear grains with high relief and cross fractures) to microcrystalline aggregates of serpentine (clear bands). Several hornblende grains (pleochroic, light grey) occur in center. The arrow marks a  $10\mu\text{m}$  grain of diopside. Dark grains are magnetite. GGU 84468. 1 mm across.
- b: Hornblende (grey) grains, microcrystalline aggregates of tremolite (white) and magnetite (black). GGU 84465. 1 mm across.
- c: Large subidiomorphic grains and fine granules of chromite in both amphibole (grey, at top) and orthopyroxene (white, at bottom). GGU 84497. 0.6 mm across.
- d: Chromite grains within and between plagioclase and biotite grains in a chromitite. The chromite grains may be cumulus, and the biotite grains probably are metasomatic. GGU 132037. 0.6 mm across.
- e: Olivine-hornblende rock with isolated coarse grains of magnetite along silicate grain boundaries and a finer-grained population within the silicates. GGU 84466. 0.6 mm across.

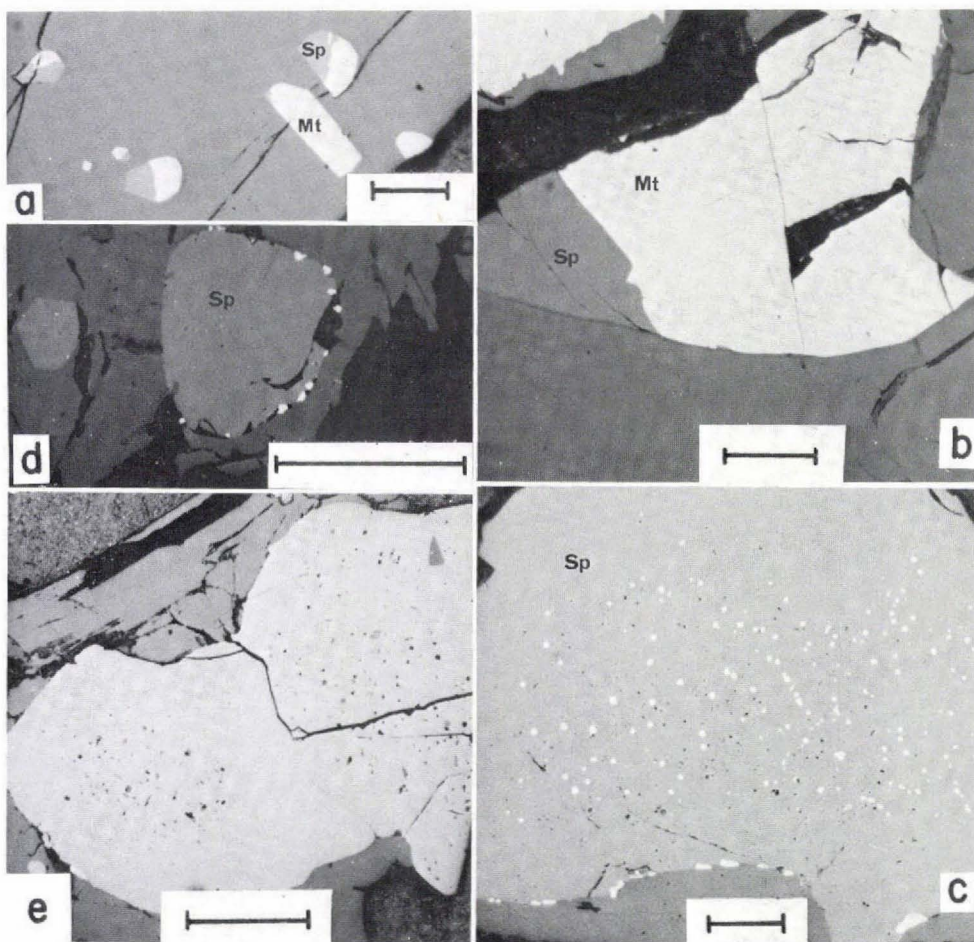


## Plate 2

Scale bar 0.1 mm.

- a: Magnetite (white) – spinel (light-grey) intergrowth in silicate host. GGU 81234.
- b: Magnetite (white) – spinel (light-grey) intergrowth in silicate host. Oriented spinel(?) darts in magnetite. GGU 84423.
- c: Spinel (light-grey) with numerous magnetite (white) inclusions. Note larger grains of magnetite at boundary between silicate (dark-grey at bottom) and spinel; also depletion of magnetite at margins of spinel. GGU 84496.
- d: Small grains of spinel (light-grey) with light magnetite grains at silicate (dark-grey) boundary. GGU 132012.
- e: Al-chromite (light-grey) in silicate (dark-grey) matrix. Small light specks within chromite and at margins are rutile. GGU 132039.



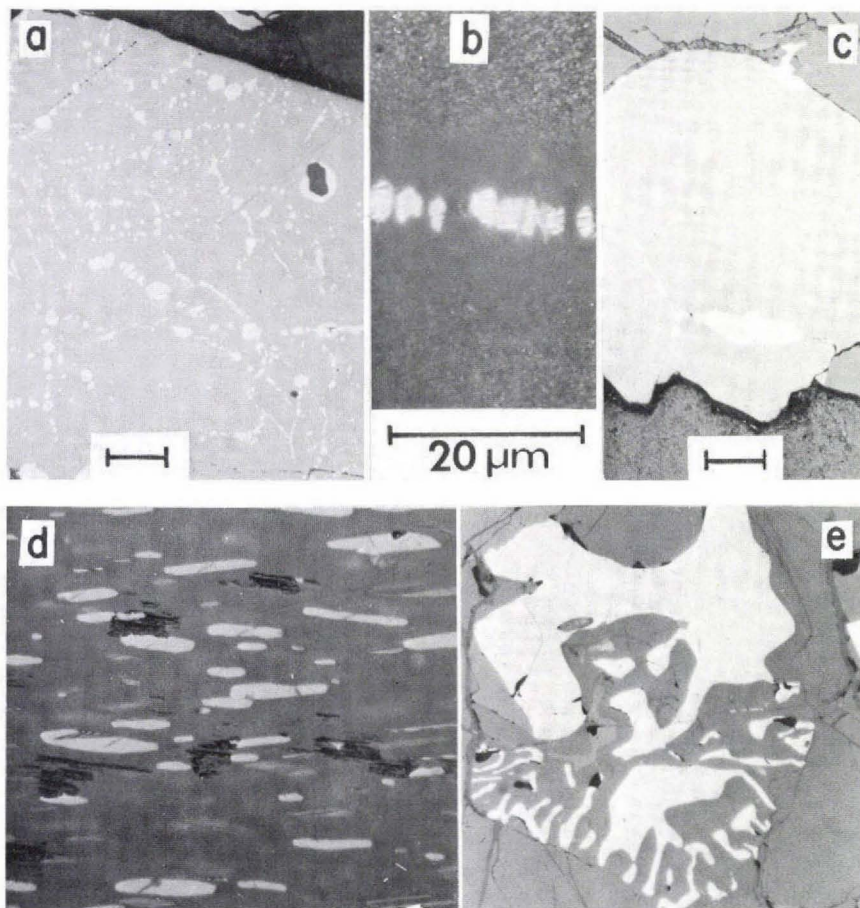



### Plate 3

- a: Al-chromite (grey) with numerous Cr-magnetite (light) inclusions. GGU 84494. Scale bar 0.1 mm.
- b: High-magnification photo of plate 3a. Oil immersion. GGU 84494.
- c: Al-chromite (light-grey) with light Cr-magnetite grains both within and at grain boundaries in silicate (dark) host. Cr-magnetite appears homogeneous at high-magnification. GGU 132012. Scale bar 0.1 mm.
- d: Cr-magnetite grains with fine spinel (?) lamellae in hornblende grain. GGU 84485. 0.2 mm across.
- e: Graphic intergrowth of magnetite and orthopyroxene. Coarse spinel lamellae (intermediate reflectivity) are present in pyroxene, and fine spinel lamellae in magnetite. GGU 84423. 0.5 mm across.

ISSN 0105-3507

 Национальная библиотека  
медицины